2010

Analysis of the Electron Withdrawing Capability of Acetylene Groups for Promoting Nucleophilic Aromatic Substitution

Eric D. Braunstein
Colby College

Recommended Citation

Analysis of the Electron Withdrawing Capability of Acetylene Groups for Promoting Nucleophilic Aromatic Substitution

Eric D. Braunstein

A Thesis Presented to the Department of Chemistry,
Colby College, Waterville, ME
In Partial Fulfillment of the Requirements for Graduation
With Honors in Chemistry

Submitted May 17th, 2010

1

Analysis of the Electron Withdrawing Capability of Acetylene Groups for Promoting Nucleophilic Aromatic Substitution
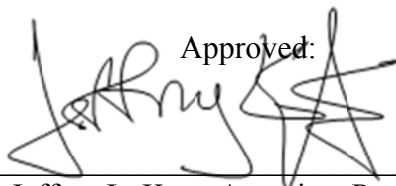
Eric D. Braunstein

Approved:

_____

(Mentor: Dr. Jeffrey L. Katz, Associate Professor of Chemistry)

May 17, 2010

_____Date

_____

(Reader: Dr. Dasan M. Thamattoor, Associate Professor of Chemistry)

May 17, 2010

_____Date

2

VITAE

Eric Daniel Braunstein was born December 17, 1987, to Frederick M. and Martha Ruth Braunstein in Albany, New York. Eric was raised in Delmar, New York, and attended Bethlehem Central High School. It was at high school that Eric discovered his passion for chemistry, and set out toward college with the goal of pursuing that field.

Eric matriculated to Colby College, in Waterville, ME, and began working in the Katz Research Group in the fall of his junior year. He continued his work in the Katz Group through the summer and his senior year, culminating in an Honors Thesis. In May 2010, Eric completed his Bachelors of Arts Degree with a Chemsitry-A.C.S. major including Honors in Chemistry, and a minor in Mathematics. He was also honored with an election to Phi Beta Kappa during his senior year.

In addition to his love of chemistry, Eric is also an avid string bassist and bass guitarist. During his time at Colby, he has performed with the Colby Symphony Orchestra, Jazz Band, Wind Ensemble, Theater Department, Broadway Musical Review, and Powder and Wig. Eric also enjoys bicycling and skiing.

Eric plans to attend Columbia University College of Physicians and Surgeons, pursuing an M.D., starting in the fall of 2010. His eventual goal is to become both a practicing physician and a medical researcher.

TABLE OF CONTENTS

TABLE OF FIGURES

ABSTRACT

It is well known that electron withdrawing groups, such as nitro or carbonyl groups, activate benzene rings for nucleophilic aromatic substitution. However, little research has been done to investigate the electron withdrawing capability of acetylene groups for substitution of aromatic halides. Experimental and computational investigations on the reactivity of halogenated phenylacetylenes with oxygen and other nucleophiles will be described.

1. INTRODUCTION

1.1 Nucleophilic Aromatic Substitution

The substitution reaction, a reaction in which one atom is replaced by another, is one of the most fundamental reactions in organic chemistry, and is of prime importance in synthesis.[1] The nucleophilic aromatic substitution reaction, a type of substitution reaction taking place on an aromatic ring, is likewise important in many syntheses. In nucleophilic aromatic substitution (S_NAr), a halogen (usually fluorine or chlorine) or another leaving group on an aromatic system is replaced by a nucleophile. In order for S_NAr to proceed, an electron withdrawing group (EWG) must be present *ortho* or *para* to the leaving group.[1] A number of electron withdrawing groups are known; however, it is generally regarded that nitroaromatics are the best reactants for S_NAr because of the high electron withdrawing capability of the group. Other EWGs such as cyano (nitrile), acetyl, and trifluoromethyl are also known to promote reactivity.[2]

Nucleophilic aromatic substitution reactions can proceed through a number of mechanisms, including aromatic S_N1 encountered with diazonium salts, benzyne (elimination-addition), as well as several transition metal catalyzed substitutions using metals such as copper and palladium. However, the reaction that will be the focus of our discussion is the traditional addition-elimination mechanism. In this two-step mechanism (Scheme 1), a nucleophile such as methoxide first adds into an aromatic system forming a resonance stabilized anionic intermediate known as a Meisenheimer complex. In the second step, the halogen is eliminated from the intermediate, rearomatizing the system and forming the substitution product.

As mentioned previously, an electron withdrawing group is essential to the progress of this reaction. The necessity of an EWG is usually explained through stabilization of the transition state, which closely resembles the anionic Meisenheimer complex intermediate. The rate of

reaction is proportional to the activation energy barrier, or the difference in energy between the starting materials and the intermediate. If the activation energy is too high, the reaction is prevented; by lowering the activation energy, we increase the rate and allow the reaction to occur. An EWG is able to lower the energy of the intermediate by providing inductive or resonance stabilization of the anionic intermediate. In the case of a nitro EWG, we explain that the resonance form with the anion residing on the two oxygen atoms is the predominant resonance form, and that because these oxygen atoms are electron poor in the neutral form of the molecule, the anionic intermediate is especially stable.
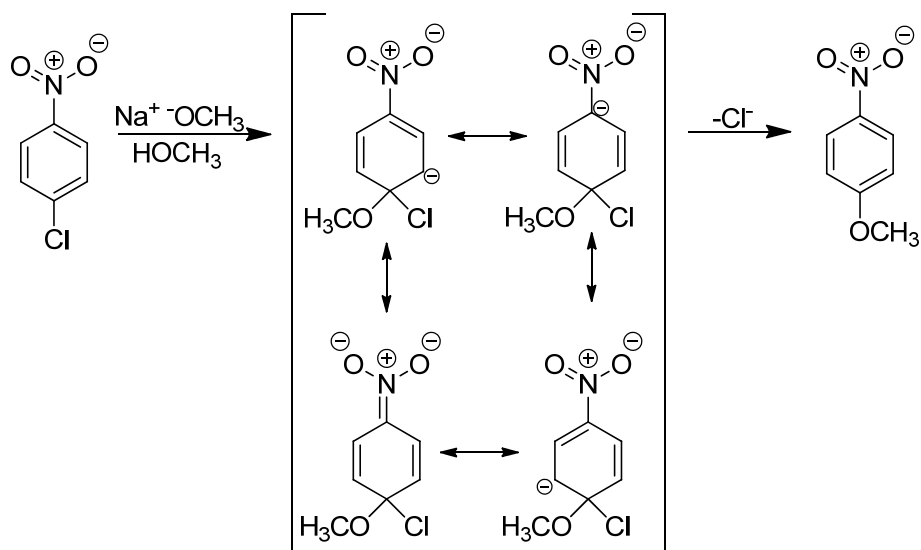
Scheme 1: The S$_N$Ar reaction mechanism with a nitro electron withdrawing group.

Using the same reasoning, we can also justify the susceptibility of aromatics bearing nitrile EWGs to S$_N$Ar. (Scheme 2) In this mechanism, we explain that the resonance form with the anion residing on the nitrogen atom stabilizes the intermediate due to the electronegativity of nitrogen, especially sp-hybridized nitrogen. Although we would not expect this stabilization to be of the same magnitude of the stabilization offered by a nitro EWG (and in fact it is not), it is still enough to promote reactivity toward substitution.
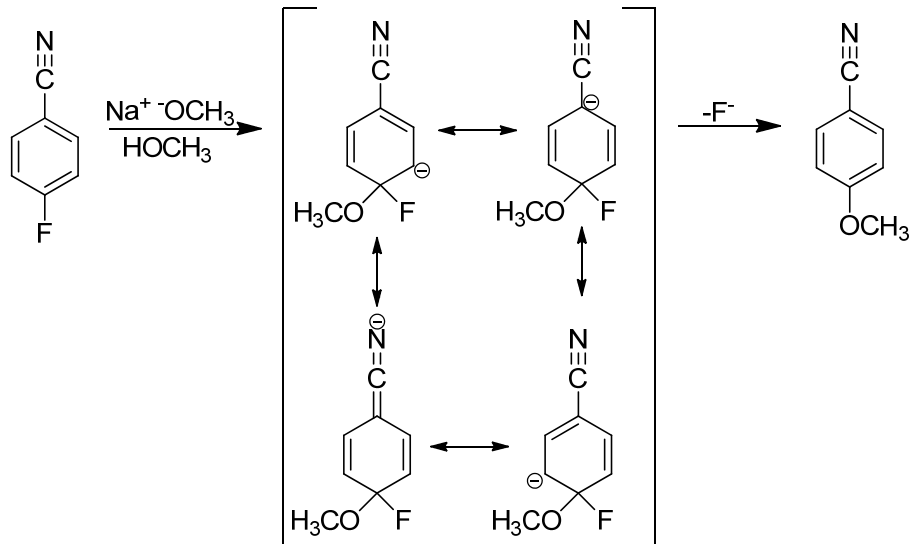
Scheme 2: The S$_N$Ar reaction mechanism with a nitrile electron withdrawing group.

1.2 Acetylene Groups

Acetylene groups (also known as alkynes), consist of two triply bound carbon atoms. Acetylenes have long been regarded as synthetically useful for construction of molecular architecture because of the variety of reactions that can be easily performed on them. Acetylenes can undergo addition by electrophiles, oxidation, and reduction (with known regiochemistry),[3] as well as undergo 2,3-dipolar cycloaddition with an azide to form a 1,2,3-triazole (click chemistry).[4] Terminal acetylenes can also be coupled to other acetylenes via Glaser[5] or Hay[6] coupling, or coupled to a halogen bearing aromatic system via Sonogashira coupling.[7] Acetylides also can act as nucleophiles for substitution reactions.[8]

1.3 Acetylene as an Electron Withdrawing Group for S_NAr

Only limited literature precedents identify acetylenes as sufficiently electron withdrawing to promote S_NAr. In 1993, it was shown that two para fluorine atoms on a diphenylacetylene could be displaced by phenoxide in a polar aprotic solvent at high temperature in "quantitative" yield.[9] (Scheme 3)
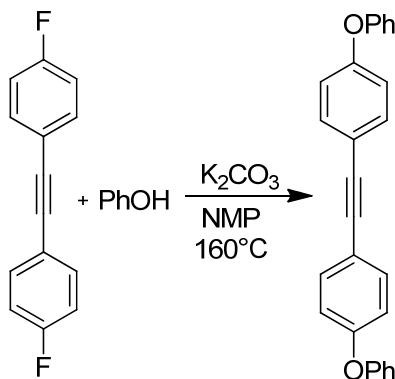
Scheme 3: A literature S_NAr reaction with an acetylene EWG.

Analyzing an S_NAr reaction with an acetylene electron withdrawing group is almost identical to analyzing a reaction with a nitrile EWG (Scheme 2). By replacing all nitrogen atoms with carbon atoms (Scheme 4), we can see that the largest difference between the two mechanisms is the placement of the anion on the sp-hybridized carbon that replaced the sp-hybridized nitrogen in resonance form **3**.
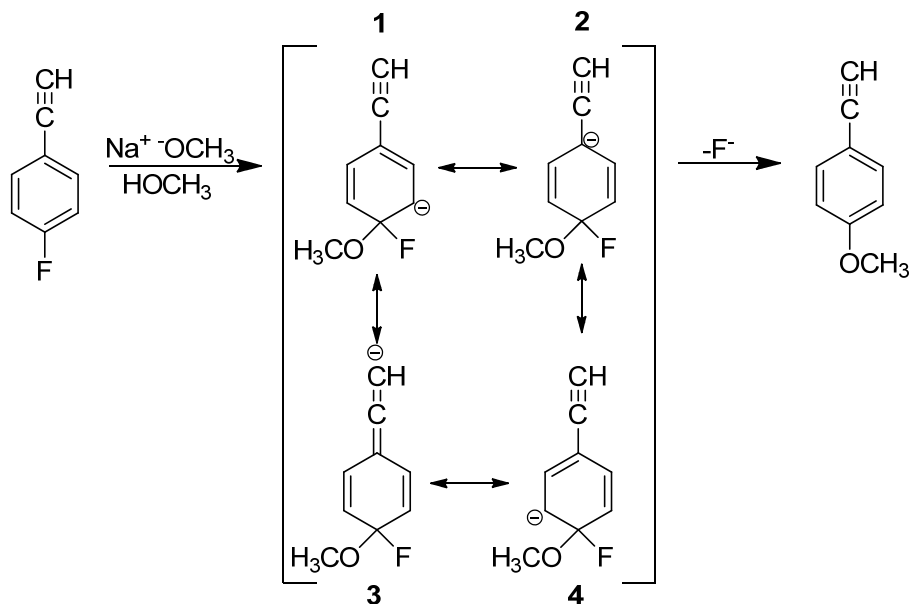
Scheme 4: The S_NAr reaction mechanism with an acetylene electron withdrawing group.

Electronegativity is often used to help determine the stability of excess charge on an atom. By comparing the electronegativity of carbon and nitrogen, we may be able to gain some insight into the electron withdrawing nature of a nitrile vs. that of an acetylene. On the Pauling scale, the electronegativity of nitrogen is 3.04, while carbon is only 2.55. While 2.55 and even 3.04 may not seem high enough to suggest much anion stabilizing ability, if we look at the Mulliken-Jaffé scale (Table 1), which tries to take hybridization into account by looking at the ionization energy and electron affinity of the elements in various oxidation states, we find that sp-hybridized carbon has an electronegativity of 3.29 and sp-hybridized nitrogen has an electronegativity of 5.07, both substantially higher than on the Pauling scale; this helps explain the high electron withdrawing ability of nitrile groups, and suggests that acetylene might have similar, albeit smaller, withdrawing ability.[10]

Table 1: The electronegativities of selected period 2 elements on the Pauling and Mulliken-Jaffé scales.

Scale	Hybridization	C	N	O	F
Pauling	-	2.55	3.04	3.44	3.98
Mulliken-Jaffé	"s"	4.84	6.70	8.98	10.31
	"p"	1.75	2.65	3.49	3.9
	sp^3	2.48	3.68	4.93	-
	sp^2	2.75	4.13	5.54	-
	sp	3.29	5.07	-	-

In reality, the stability of the Meisenheimer complex is dependent on the ability of the whole molecule to support negative charge, not just one atom in one resonance structure. An analogy can also be made by analyzing the inductive anion stabilizing ability of trifluoromethyl EWGs. Trifluoromethyl is described as having an electron withdrawing effect due to the positive polarization caused by the three polar fluorine-carbon bonds. Likewise, the ethynyl group also has three bonds (one sigma and two pi) to a relatively electronegative atom, carbon. Between the small amount of precedent and our reasoning using these two analogies, it appears that additional research into the electron withdrawing nature of acetylenes is warranted.

1.4 Analyzing Electron Withdrawing Capability Using Rates and the Hammett Equation

When comparing the electron withdrawing capability of functional groups for S_NAr, what we are really comparing is the rate of the substitution reaction on systems with different substituents. Although direct comparison of rates can be useful to a synthetic organic chemist, it is limited in that it only gives information about the reaction being studied. In order to quantitatively generalize the electron withdrawing effect to a range of reactions, we can use the Hammett equation. In 1937, Louis Hammett developed the Hammett equation; in its simplest form, it is written:

$$log \frac{k}{k_0} = \sigma\rho \qquad\qquad (1)$$

where k is the rate constant of the reaction of interest,[a] k_0 is the rate constant of a reference reaction, σ is the substituent constant, and ρ is the reaction constant. In his work, Hammett showed that for 38 different reactions involving 31 different substituted benzene molecules, the rate could be related to the two aforementioned constants using this equation. He proved that the substituent constant only depended on the substituent on the benzene ring, and that the reaction constant only depended on the type of reaction that was being studied.[11]

Despite Hammett's initial postulate, it has been found that one set of substituent constants is not sufficient for all types of reactions. Besides the σ_m and σ_p values that Hammett himself proposed for para and meta substituents (assuming ortho and para would display similar reactivity ignoring steric effects), there are also references in literature to σ^- and σ^+ values, for reactions involving anionic and cationic intermediates respectively, as well as several other more esoteric σ values. For S_NAr, and specifically for the reactions we propose to study, we looked at literature σ_p^- values as a starting point. Because S_NAr proceeds through an anionic intermediate, a σ^- value was deemed most appropriate, and para substituted substituents were studied first.

In 1969, Colin Eaborn et. al. studied the reactivity of phenylacetylenes by looking at reactions of substituted phenyl and benzyl stannanes. He measured σ_p^- values through rates of alkali cleavage of p-ethynylbenzyltrimethyl–silane and –stannane, (Scheme 5) and determined a value of σ_p^- for the ethynyl group as 0.52 and 0.53.[12]

---

[a] The Hammett equation was actually originally written using equilibrium constants (K) instead of rate constants (k), but it is now accepted that it can be used either way.
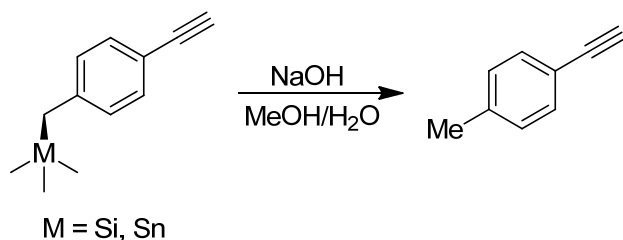
Scheme 5: The alkali cleavage reaction of p-ethynylbenzyltrimethyl–silane and –stannane used for finding σ_p^-.

Otto Exner also reported the σ_p^- value for the ethynyl group as 0.52, only slightly less than that of trifluoromethyl at 0.62.[13] This is promising, as trifluoromethyl is a documented EWG that allows S_NAr to occur. Interestingly, the reported σ_p^- values for phenylacetylene are 0.39[13] and 0.30,[14] less than for the ethynyl group. This is opposite of what we would expect for S_NAr because of the known electron withdrawing nature of a phenyl group ($\sigma_p^- = 0.08$), and this brings to point the method by which these values were calculated. Although Eaborn's reactions of stannanes and silanes are anionic in nature, the intermediate is quite different from the Meisenheimer complex seen in S_NAr, and thus these values may not hold true for S_NAr.

2. DISCUSSION

2.1 Sonogashira Coupling

Sonogashira coupling is a palladium and copper catalyzed cross-coupling reaction that can be used to create a carbon-carbon bond between an aryl or vinyl halide and a terminal alkyne. (Scheme 6) The halogen must be one of the heavy halogens (I>Br>Cl, in terms of rate), but the reaction is very versatile with respect to the aromatic system and the alkyne. Sonogashira coupling was used to generate several of the S_NAr reaction precursors.
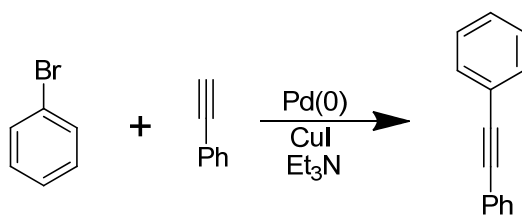
Scheme 6: A prototypical Sonogashira coupling reaction.

Although the reaction mechanism for Sonogashira coupling is not fully understood, it is thought to involve two interconnected catalytic processes: One in which copper(I) reacts with the terminal acetylene to form a copper(I) acetylide, and one in which Pd(0) first inserts oxidatively into the aryl-halogen bond, then ligand exchange or metal metathesis occurs to form a Pd-acetylide, followed by product formation via reductive elimination. (Scheme 7)

Pd(0) complexes commonly used for Sonogashira coupling, such as tetrakis(triphenylphosphine)palladium(0), are readily susceptible to degradation by even trace amounts of atmospheric oxygen, and thus must be used in a glove box. This degradation can occur in two ways; the triphenylphosphine ligands can be oxidized to triphenylphosphine oxide, causing the ligandless Pd(0) to turn into colloidal bulk palladium, or palladium black, which is inactive as a catalyst. The Pd(0) can also be directly oxidized to PdO, which is also inactive as a catalyst. In order to get around the glove box requirement, air-stable Pd(II) complexes can be

used as catalyst precursors, and reduced *in situ* to Pd(0). In the Sonogashira coupling reactions that follow, bis(triphenylphosphine)palladium(II) dichloride was used as a palladium source. This complex is reduced through reductive elimination by the terminal alkynes in the reaction solution to form Pd(0) and the symmetric bisacetylene, *vide infra*. Because the terminal alkyne is used to reduce the Pd(II) precatalyst, it is important to keep catalyst loading low to reduce the amount of the bisacetylene byproduct.
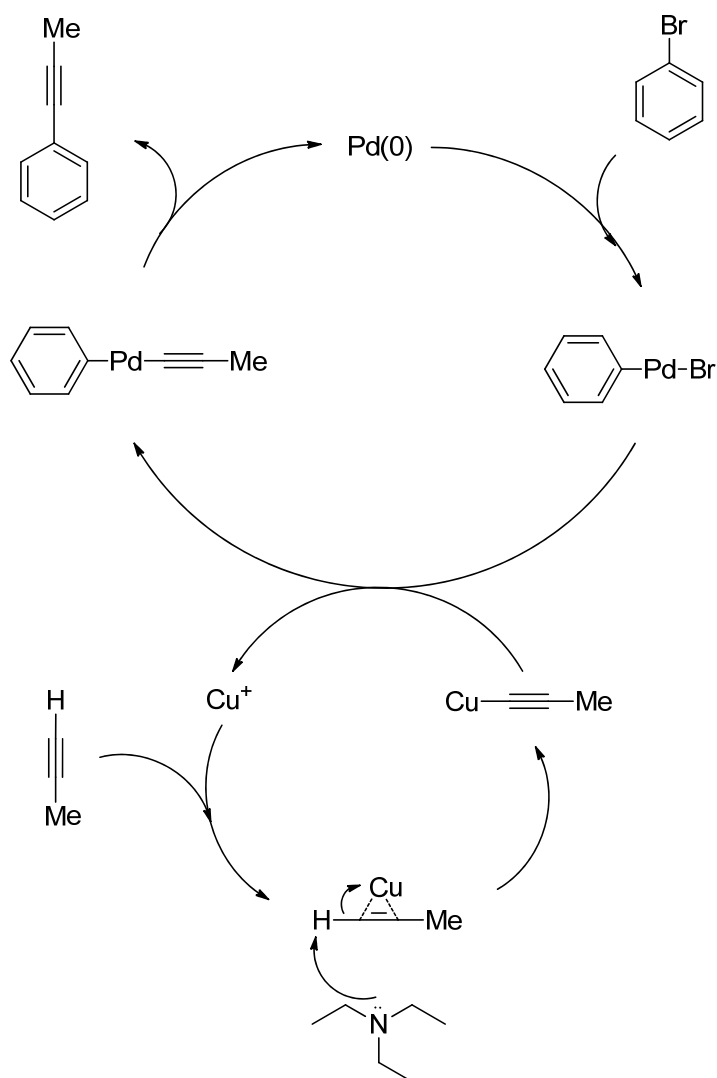
Scheme 7: The Sonogashira coupling reaction mechanism.

Besides the acetylene-acetylene coupling resulting from Pd reduction, a similar process can also occur called Glaser coupling. Glaser coupling is a Cu(I) catalyzed coupling of two terminal alkynes to form the symmetric biacetylene. (Scheme 8) Glaser coupling relies on stoichiometric oxygen to oxidize the copper in the catalytic cycle, so it will only occur if oxygen is present in the reaction solution. As mentioned previously, oxygen can also degrade Pd(0) complexes, and this is equally true of Pd(0) produced *in situ* from Pd(II). For these reasons, it is imperative to use rigorous Schlenk techniques to avoid oxygen contamination.

$$2 \ \ Ph \!-\!\!\equiv \quad \xrightarrow[\text{Et}_3\text{N, O}_2]{\text{Cu(I)}} \quad Ph \!-\!\!\equiv\!\!-\!\!\equiv\!\!-Ph$$
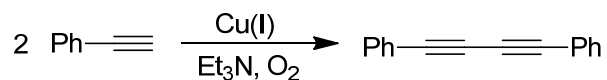
Scheme 8: A prototypical Glaser coupling reaction.

Sonogashira coupling reactions were used to generate a variety of phenylacetylenes that were used for S_NAr reactions. Phenylacetylenes **1-4** were generated in 48-70% yield.
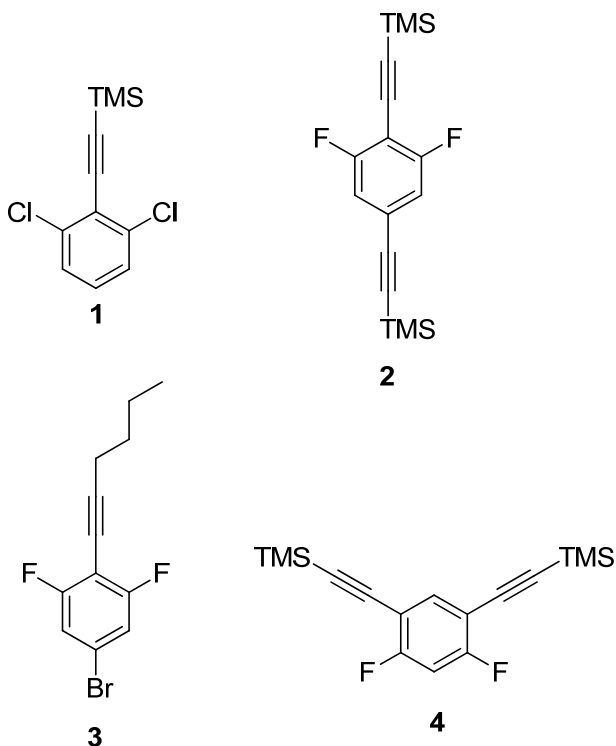
2.2 Solvent and Base Effects in S_NAr

Several different solvents are suitable for S_NAr reactions of the type that were performed. S_NAr reactions are accelerated by use of polar solvents, which stabilize the anionic Meisenheimer complex intermediate; however, besides the requirement of polarity, any number of solvents, both protic and aprotic, can be used. S_NAr reactions have been shown successful in water, alcohols (methanol, ethanol, etc.), amines (pyridine, triethylamine, Hünig's base), acetonitrile, THF, HMPA, NMP, DMSO, DMF, and even more non-polar solvents like toluene and dioxane.[15] For the following investigations, primarily aprotic polar solvents were used, which tend to maximally accelerate the reactions. DMSO was by far the most commonly used solvent in the experiments, but DMF, NMP, and ethanol were also used at various points. Of these solvents, reactions using oxygen and nitrogen nucleophiles were found to be the fastest in DMSO, which follows with it having the highest dipole moment and dielectric constant of the solvents screened.

A variety of bases also can be used to promote S_NAr reactions, and base choice is largely dependent on the type of nucleophile being used. Oxygen nucleophiles (alcohols and phenols) need to be deprotonated to form alkoxides or phenoxides in order to be reactive toward S_NAr reactions. Alcohols are less basic than phenols, and therefore need to be deprotonated with a strong base like NaH. For phenols, there are a variety of bases, including potassium carbonate (K_2CO_3), cesium carbonate ($Cs_2CO_{3)}$, cesium fluoride (CsF), and potassium *tert*-butoxide (*t*-BuOK), that will perform the deprotonation. K_2CO_3 and Cs_2CO_3 have similar basicity in solution; however, the larger counter-ion in Cs_2CO_3 gives it better solubility in organic solvents than K_2CO_3. CsF and Cs_2CO_3 are both relatively weak bases in water, but display very different base strength in DMSO. Carbonic acid has a pKa of 10.33 in water, but closer to 25 in DMSO.

Likewise, hydrofluoric acid has a pKa of 3.17 in water, but 15 in DMSO.[16] For comparison, the pKa of *p*-cresol, the species that needs to be deprotonated, in DMSO is 18.9.[17]

Nitrogen nucleophiles often are reactive enough in their neutral form to perform substitution, and a relatively weak base such a tertiary amine can be used merely to scavenge protons after the substitution has occurred. In the case of electrophiles with acetylene EWGs, substitution with neutrally charged nitrogen nucleophiles was too slow to occur even at high temperatures. In such cases sodium hydride was used to deprotonate the amine to form an anionic amide, which was very reactive toward the electrophiles.

The choice of optimal base to use in S_NAr reactions with phenol nucleophiles was paramount to the rate studies that follow, as a substituted phenol was used as the nucleophile. For kinetic experiments, it is essential that the concentration or the active species (in this case, the phenoxide anion) be known; therefore, it had to be ensured that all phenol in solution was deprotonated, and that the solution was homogeneous. CsF and Cs_2CO_3 both led to problems as their base strength is not high enough to ensure complete deprotonation, and they are not fully soluble in DMSO, leading to non-homogeneous solutions. Instead, *t*-BuOK, (*t*-BuOH has a pKa in DMSO of 32.2),[18] was used for rate studies as it allowed for complete deprotonation of the phenol, as well as homogeneous reaction solutions.

2.3 Rate Studies of S_NAr with several EWGs

The S_NAr reactions considered in this study proceed through a 2-step addition-elimination mechanism. The addition step follows attack of the nucleophile on the electrophilic π-system to form an intermediate Meisenheimer complex. This is followed by elimination of the

halogen to form the substitution product. In most cases, including this study, the addition step is rate-determining.

As a bimolecular reaction, S_NAr should follow standard second order kinetics, with the rate defined as:

$$rate = k\,[Nu]\,[E] \tag{2}$$

Where k is the second-order rate constant (in $L \cdot mol^{-1} \cdot s^{-1}$), $[Nu]$ is the concentration of nucleophile, and $[E]$ is the concentration of electrophile (both in M). By integrating and rearranging, we can yield two new equations:

$$[E] = \frac{(Nu_0 - E_0)}{\frac{Nu_0}{E_0} e^{(Nu_0 - E_0)kt} - 1} \tag{3}$$

$$[Nu] = \frac{(E_0 - Nu_0)}{\frac{E_0}{Nu_0} e^{(E_0 - Nu_0)kt} - 1} \tag{4}$$

Where E_0 is the initial concentration of electrophile, Nu_0 is the initial concentration of nucleophile, and t is time (in seconds). These equations rely only on having known initial concentrations of reactants, so if these are found, we can use non-linear curve fitting to fit experimentally determined time-dependent concentration data to k, the second-order rate constant.

Initial concentration data is often determined from measured masses and volumes; however, it was decided that in this case, it would be more accurate to determine the initial concentrations using the same methodology as the time-dependent concentrations, by NMR.

NMR is a powerful technique not only for determining molecular structure, but also for determining concentrations of species in a solution. Integrations of ^1H NMR signals are proportional to concentration of the species in the solution as long as the protons are allowed to

fully relax. Concentrations of species in solution were determined by comparing the integrations of the nucleophile and electrophile signals to the integration of an internal standard that was added to the solvent. Because the concentration of the internal standard was known, we could calculate the concentrations of the reactants by normalizing against the standard. The standard used was 1,3-dimethyl-2-imidazolidone (DMI), a cyclic urea that is also sometimes used as a polar aprotic solvent. Because this standard is similar in solvating ability to the solvent (DMSO), is inert under the reaction conditions, and was present in low concentration, it was hypothesized it would not affect the rate of reaction significantly.

When running reactions where rate is to be determined, it is essential that concentrations are determined accurately. For this reason, a number of steps were taken to maximize the precision and accuracy of results. Since some of the reactants used in the reactions were relatively volatile, reactions were run in sealed containers to prevent losses of reactants due to evaporation. Transferring reactants from the reaction solution to a deuterated solvent for NMR measurements was also an issue. After testing a variety of methods, it was determined that small aliquots would be taken from the reaction solution at known times, and quenched with HCl to ensure no further reaction would take place. The aliquots were then extracted from the HCl with $CDCl_3$, which was transferred directly to an NMR tube for spectroscopic measurement. Solvent evaporation *in vacuo* was avoided again because of the volatility of the reactants. Although the extraction procedure could lead to some loss of reactants in the aqueous acid layer, it was determined that loss was minimal, although this could be a source of error in the procedure.

Once time-dependent concentration data was acquired, it was fit to the two integrated rate equations using the solver add-in for Microsoft Excel. Standard deviations in the fit parameter were found using the SolverAid macro developed by Robert de Levie.[19]

Rate studies were performed on *para*-substituted fluorobenzenes **5-10** by reacting them with *p*-cresol **11**. (Scheme 9) All studies were performed at 85 °C, which was chosen because it allowed for measurements of all rates in reasonable time frames. It was important that all reactions be run at identical temperatures as the rate constant is temperature dependent. Temperature fluctuations are also a likely source of error in the measurements of *k*; maintaining a reaction vessel at exactly 85 °C for long periods of time is difficult, with fluctuation of up to ±2 °C possible.
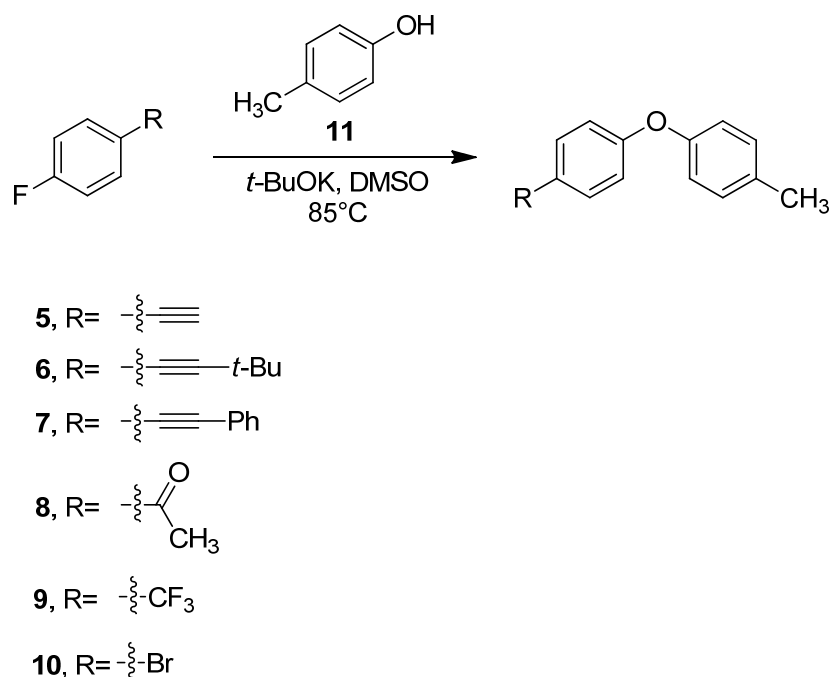
Scheme 9: Rate studies of *para*-substituted fluorobenzenes.

Results of rate studies are summarized below (Table 2). Values for *k* are the arithmetic mean of all *k* values determined from non-linear least squares curve fitting. Error in k is % standard deviation (1 σ), found by simply determining the standard deviation of the fit parameters, but ignoring the error in the fit as determined by SolverAid. Although ignoring the error in the fit is not statistically sound, we were unable to perform proper error analysis because of the small size of our data set, so the standard deviation can be used as a reference.

Table 2: Summary of rate data for kinetic studies.

Electron Withdrawing Group	k (L·mol^{-1}·s^{-1})	Standard Deviation in k	% Error	Relative Rate
Acetyl	7.15E-03	1.53E-03	21	250
Trifluoromethyl	6.36E-04	1.54E-04	24	22
Phenylethynyl	5.59E-05	1.26E-05	23	2.0
Ethynyl	2.85E-05	6.29E-06	22	1
Bromide	3.70E-06	3.19E-06	86	0.13
tert-Butylethynyl	3.18E-06	1.02E-06	32	0.11

It was found that the ethynyl EWG is approximately 10 times more electron withdrawing than bromide, and 20 times less reactive than trifluoromethyl; this is quite a significant result, as both bromine and trifluoromethyl are known to promote S_NAr. The relative rate of phenylethynyl is about double that of ethynyl, supporting our original hypothesis that the σ_p^- value reported for phenylethynyl by Exner,[13] which was much lower than his value for ethynyl, was not reliable.

The relative rate with a *tert*-butylethynyl EWG is the same as for bromide (within error), which is notable considering the significantly higher rates of the other two tested ethynyl groups. This decrease in rate is likely due to hyperconjugative interactions of the π system with the *t*-butyl C-C bonds, as well as the inductive electron donating nature of alkyl groups.

2.4 Hammett Analysis of S_NAr rate studies.

Using the Hammett equation, $\log(k) = \sigma\rho$, as discussed in section 1.4, several plots were produced to measure the correlation between measured rates and literature σ values. Values reported by Exner[13] and Taft[14] for σ_p^- (Figure 1) and σ_p (Figure 2) were plotted against $\log(k)$. Linear least squares fitting was performed to yield a line with a slope of ρ, the substituent constant, and an arbitrary y-intercept. All measured EWGs were plotted with the exception of *t*-butylethynyl, which had no literature σ values.
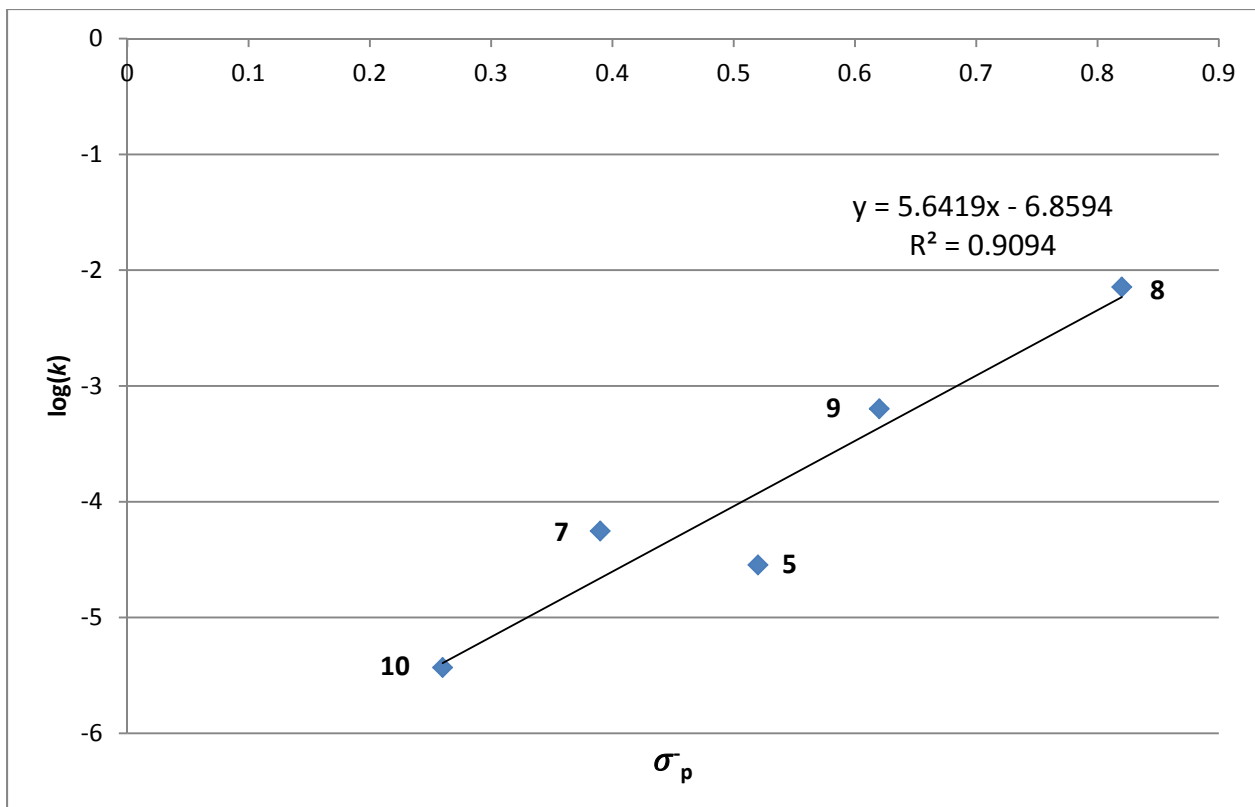
Figure 1: Hammett plot of log(k) vs σ_p^- values reported by Exner.
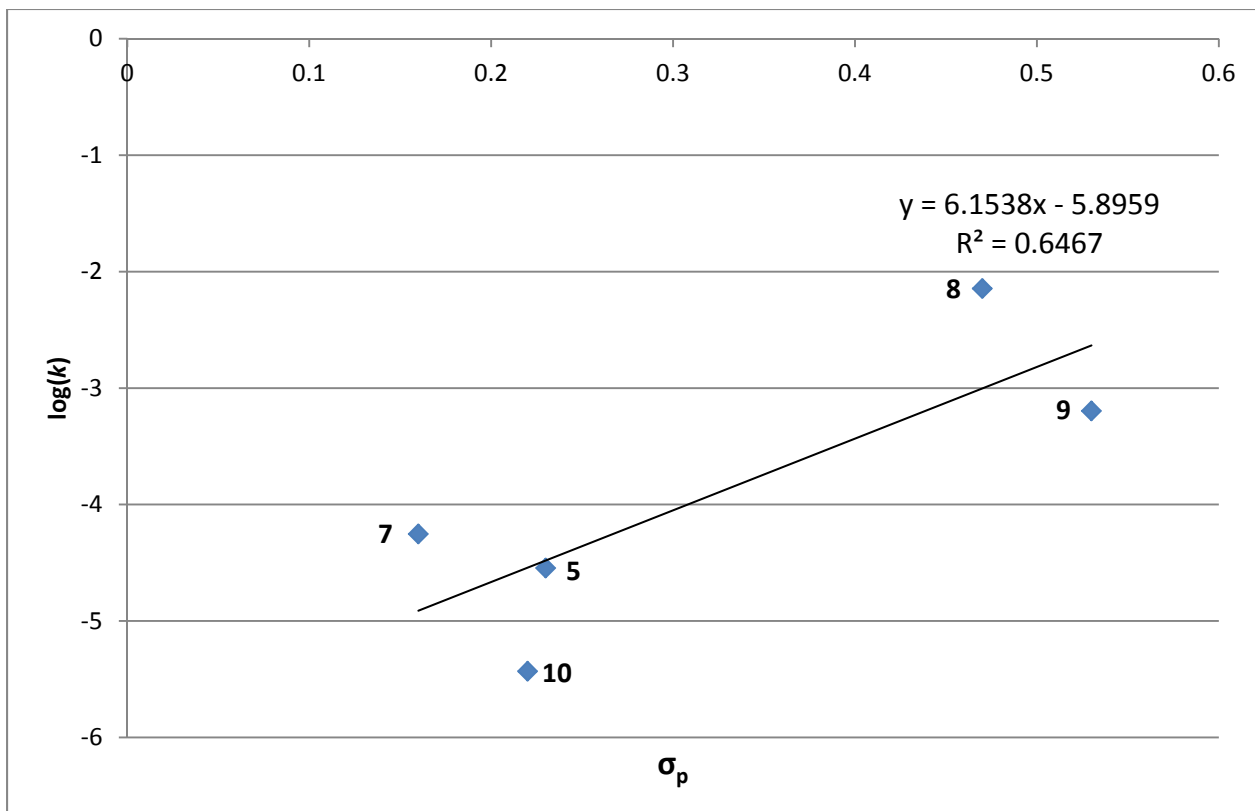
Figure 2: Hammett plot of log(k) vs σ_p values reported by Exner.

Table 3: Literature and calculated σ values.

Electron Withdrawing Group	Literature σ_p^-	Literature σ_p	Calculated σ_p^-
Acetyl	0.82	0.47	-
Trifluoromethyl	0.62	0.53	-
Phenylethynyl	0.39/0.30	0.16	0.46
Ethynyl	0.52	0.23	0.41
Bromide	0.26	0.22	-
tert-Butylethynyl	-	-	0.24

By analyzing the R^2 values of the two fits, it becomes clear that σ_p^- is much more closely correlated to the rate data, validating the hypothesis that it was the correct value to use for analysis. The two EWGs in figure 1 that are furthest from the best fit line are both ethynyl EWGs, which suggests that there values may not be correct. Another Hammett plot can be constructed using σ_p^- only from non-ethynyl EWGs. (Figure 3) This plot again yields a line with a slope of ρ. This value or ρ is similar to the value calculated using all five EWGs, so it was decided that the ρ from all five EWGs would be used. Using this calculated ρ value, we calculated three new σ values for the ethynyl EWGs, which are likely more accurate than the literature values, at least for $S_N Ar$ reactions. (Table 3)

A Hammett plot can also be constructed using the Hammett equation with a reference rate, $\log(k/k_0)=\sigma\rho$. (Figure 4) This plot maintains the same slope (and therefore ρ value) as without a reference rate, but has the traditional y-intercept of 0 for Hammett plots. In order to produce this plot, k_0 was varied to minimize the y-intercept, making it essentially 0. This value for k_0 was 1.38E-07, which may represent the rate we would see if we could "force" the reaction to proceed with hydrogen as the EWG, as the literature σ values used to produce the plots should be referenced to hydrogen with a σ value of 0.
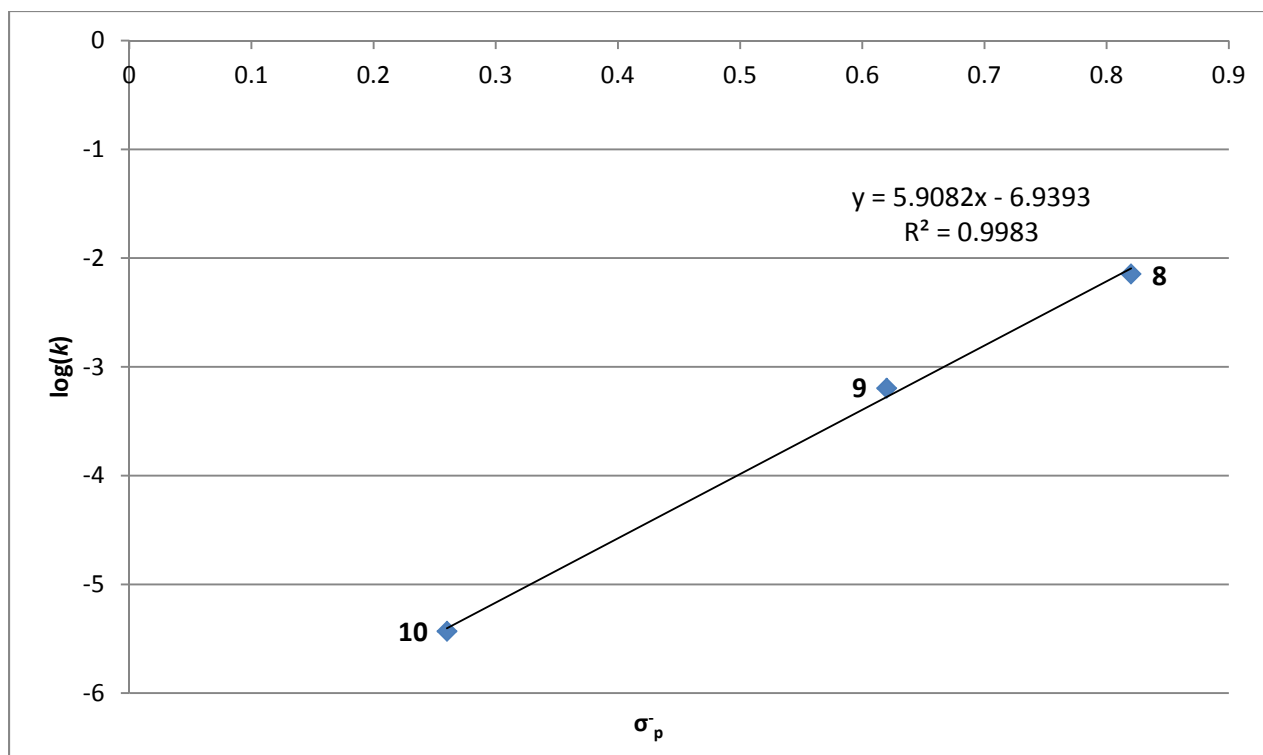
Figure 3: Hammett plot of log(k) vs σ_p^- values for non-ethynyl EWGs.
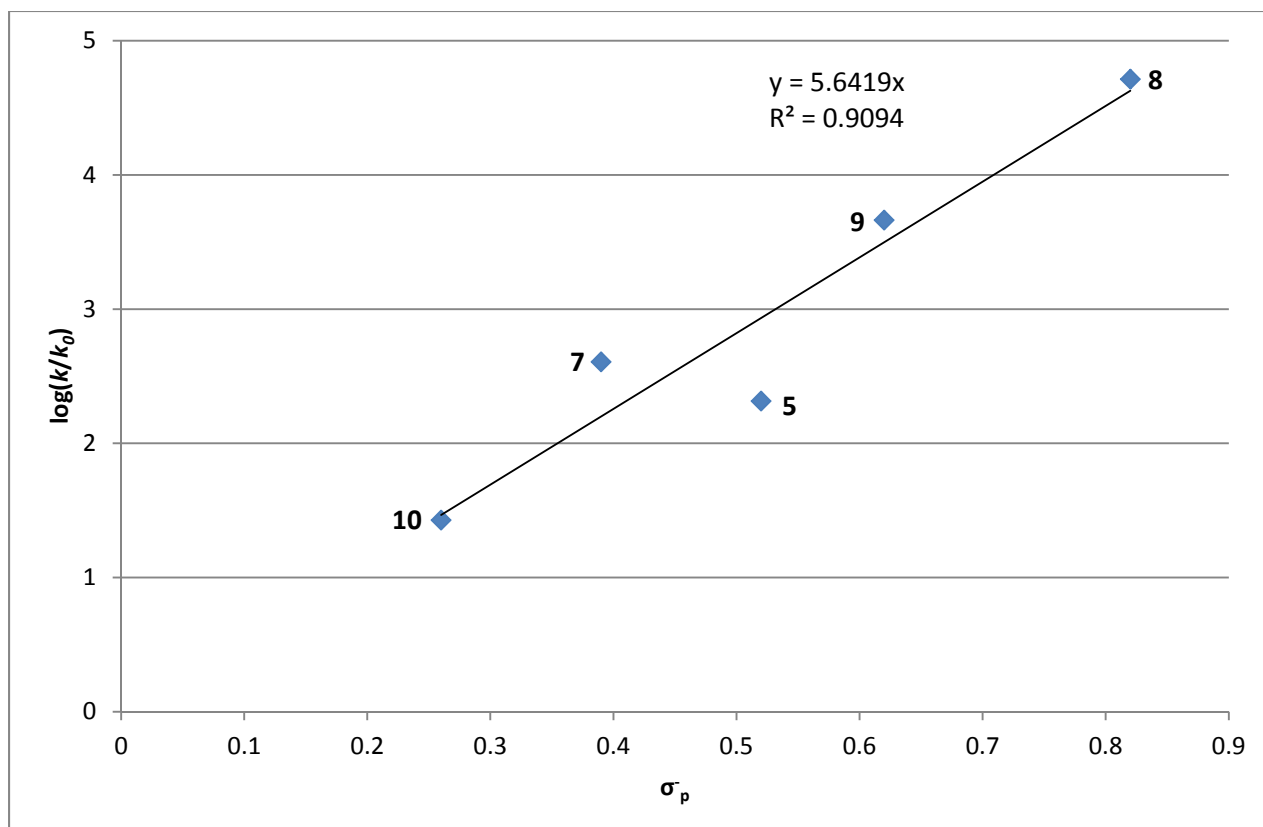
Figure 4: Hammett plot of log(k/k_0) vs σ_p^-.

2.5 S_NAr with other *ortho* and *para*, and di-substituted fluorobenzenes

Substitution reactions were performed with other *ortho* and *para*-substituted fluorobenzenes that were not included in the rate studies, leading to a number of interesting insights into the reactivity of benzenes with acetylene and other EWGs. Reaction conditions were similar to those used for kinetic studies, although temperature was adjusted based on reactivity of the electrophile.
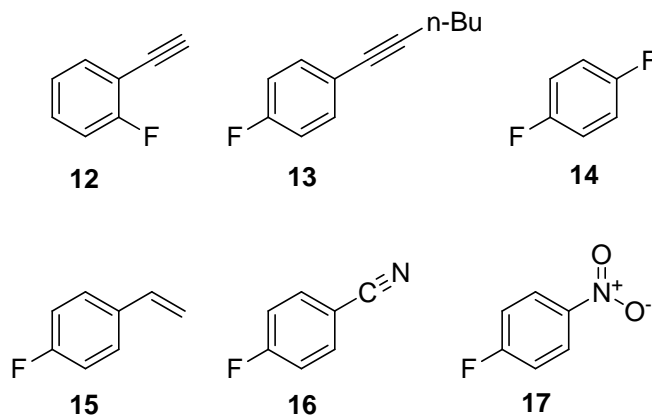
When subjected to S_NAr reaction conditions, fluorobenzene systems bearing acetylene EWGs vary in their propensity for aromatic substitution versus nucleophilic addition to the acetylene. When **12** was reacted with **11** under similar conditions to the kinetic studies (hereafter referred to as general reaction conditions), four major products **18-21** were formed in an approximately 5:6:2:1 ratio. This shows that for the *ortho*-fluoro system, addition is slightly favored, but that both reactions have fairly comparable rates. When this reaction was run in DMSO-d6, all labeled hydrogens on **18-21** were replaced by deuterium in the products, showing that some proton exchange with DMSO is possible under the reaction conditions. Likewise, when *para*-isomer **5** was reacted with **11** under general reaction conditions, small amounts of olefin **22** (as a mixture of olefin isomers) are also formed. In this case, the ratio of substitution to

addition product was very large, showing that in this system the rate of substitution is higher than the rate of addition.

18   19   20   21

22
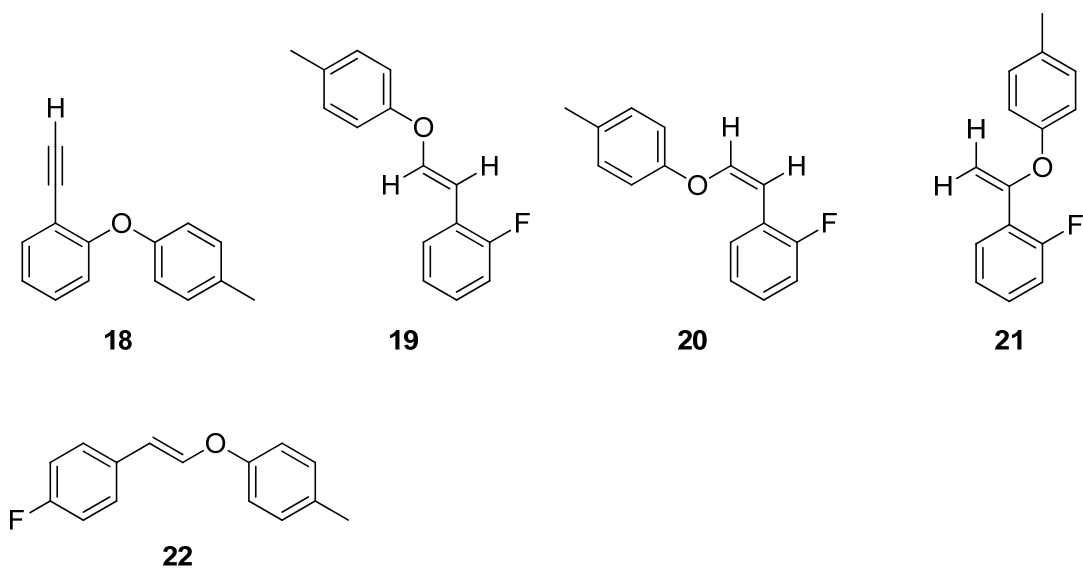
When *n*-butyl-acetylene **13** was reacted with phenol **11** under general reaction conditions, a large number of products were formed, which appeared to be structures like **23-25** as assigned by ¹H NMR. Products like these result from propargylic rearrangement down the butyl chain facilitated by deprotonation, followed by addition. Rearrangements like these are not possible with **6** because of the lack of a propargylic proton, and addition like that seen with terminal acetylenes is likely sterically blocked by the bulky *t*-Bu group.

23   24   25
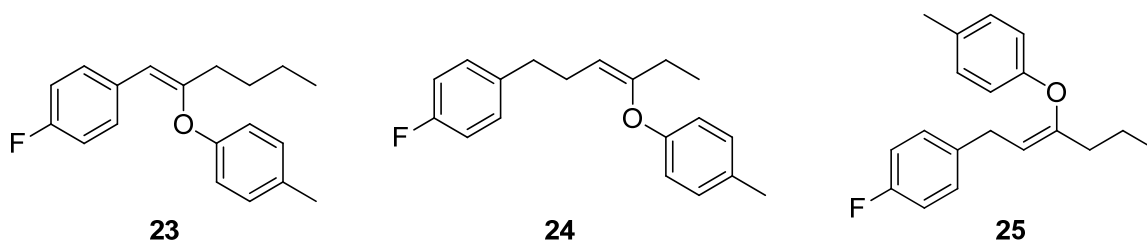
The underlying reason behind why some fluorophenylacetylenes favor substitution while others favor addition is not known, and hence it is difficult to predict the reaction that will take place for a given substrate. It has been suggested that fluorine tends to direct reactions in the

ortho as opposed to *para* position, and this helps explain why **5** favors substitution but **11** favors addition.

Fluoro- and vinyl-substituted electrophiles **14** and **15** were screened as potential candidates for kinetic studies, but neither underwent observable substitution when subjected to the general reaction conditions. No reaction was seen in **14**, while **15** appeared to undergo a polymerization reaction. Likewise, nitrile- and nitro-bearing substrates **16** and **17** were screened as candidates as well, but they both reacted too quickly under the general reaction conditions to yield reliable rate information.

Difluorobenzenes **2** and **3** were reacted with **11** in an attempt to form triaryldiethers, but the reactions failed with many side products being formed. A polymerization reaction appeared to occur with **2**, while several addition products were observed with **3**, likely due to the propargylic proton, similar to the reactivity seen with **13**.

2.6 S$_N$Ar with other nucleophiles

Substitution reactions were performed using several nucleophiles other than phenoxides in order to test the scope of reactivity of phenylacetylenes toward S$_N$Ar. When phenylacetylene **5** was reacted with hexylamine using the general reaction conditions at high temperatures (175 °C), a large number of products, which appeared to be primarily addition products, were observed. Reaction of trifluoromethyl-substituted substrate **9** with hexylamine under general reaction conditions at 160 °C showed successful substitution.

Reactions of methylamine (dissolved in ethanol) and methylamine hydrochloride were successful with methyl-ketone **8** when a weak amine base was used, but unsuccessful with phenylacetylene **5** using either amine bases or Cs$_2$CO$_3$, with no reaction seen even at 220 °C.

This is likely due to the large reactivity difference between the two electrophiles as seen in the rate studies, as well as the low reactivity of amine bases. Reaction of ethanol with both **5** and **8** proved successful at 50 °C using the general reaction conditions with a sodium hydride base, which highlights the high reactivity of alkoxide nucleophiles.

Reaction of aniline with trifluoromethyl-substituted substrate **9** under the general reaction conditions, which formed an anionic amide nucleophile, showed full conversion to the substitution product almost immediately at r.t. Likewise, reaction of aniline with **5** showed fast reactivity at r.t., but yielded a complex mixture of substitution and addition products.

2.7 Computational Results

Ab initio post-HF calculations were performed on several of the electrophiles used for kinetic studies in an attempt to find correlations of rate data with LUMO orbitals energies and activation energies.

LUMO orbital energies were analyzed by first performing geometry optimizations on electrophiles **5-10** using density functional theory (B3LYP/6-311+G(d)), then performing single point energy calculations using coupled cluster theory (CCSD/cc-pVTZ). It was thought that if the systems followed the general rule that reactions tend to be HOMO/LUMO interactions, then the LUMO energy would correspond to the rate of reaction, with lower energies corresponding to higher rates. The LUMO, which generally had a configuration similar to those seen in figures 5-6 for all modeled electrophiles, was thought to be the reactive orbital because of the orbital density on the fluorine bearing carbon. In the case of **10** the orbital with this general configuration was the LUMO+1. These LUMO energies, once calculated for all systems, were found to have little correlation to rate (Figure 7).
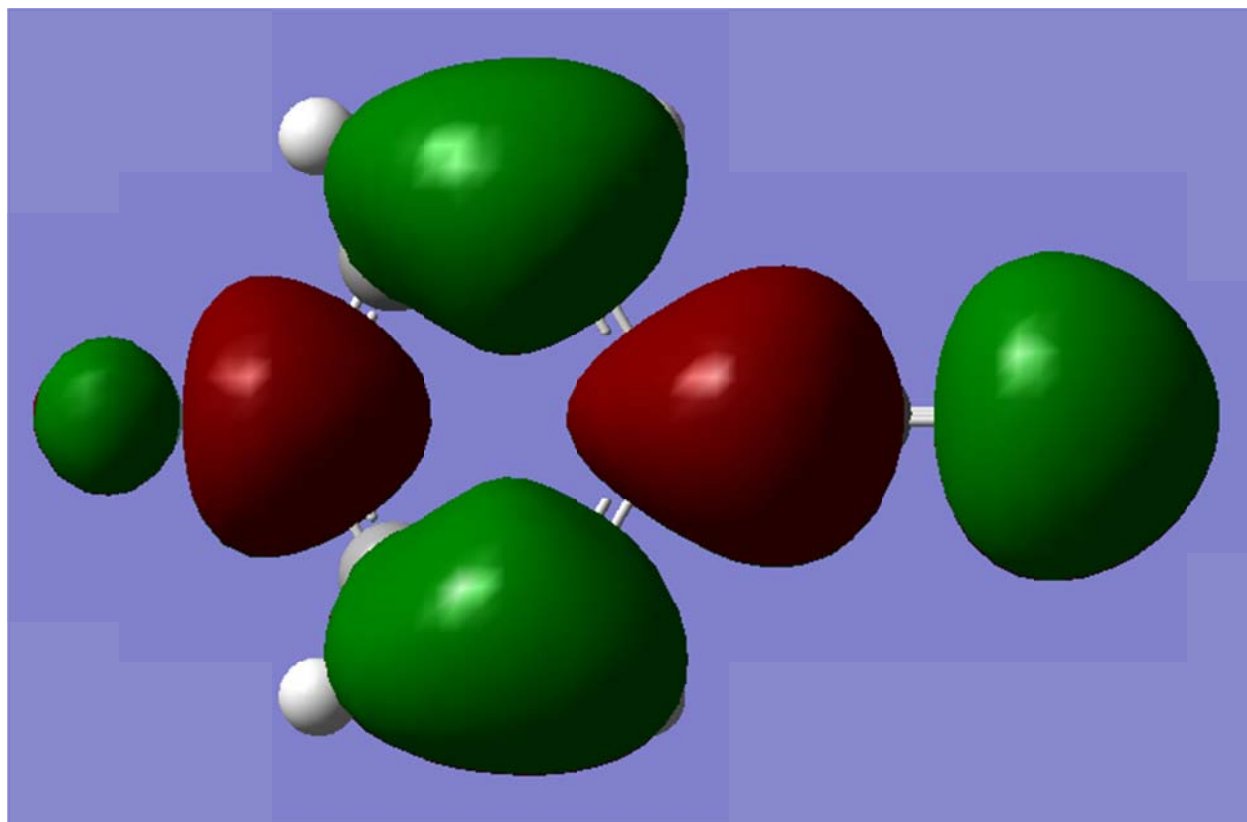
Figure 5: LUMO of 5 at CCSD/cc-pVTZ.
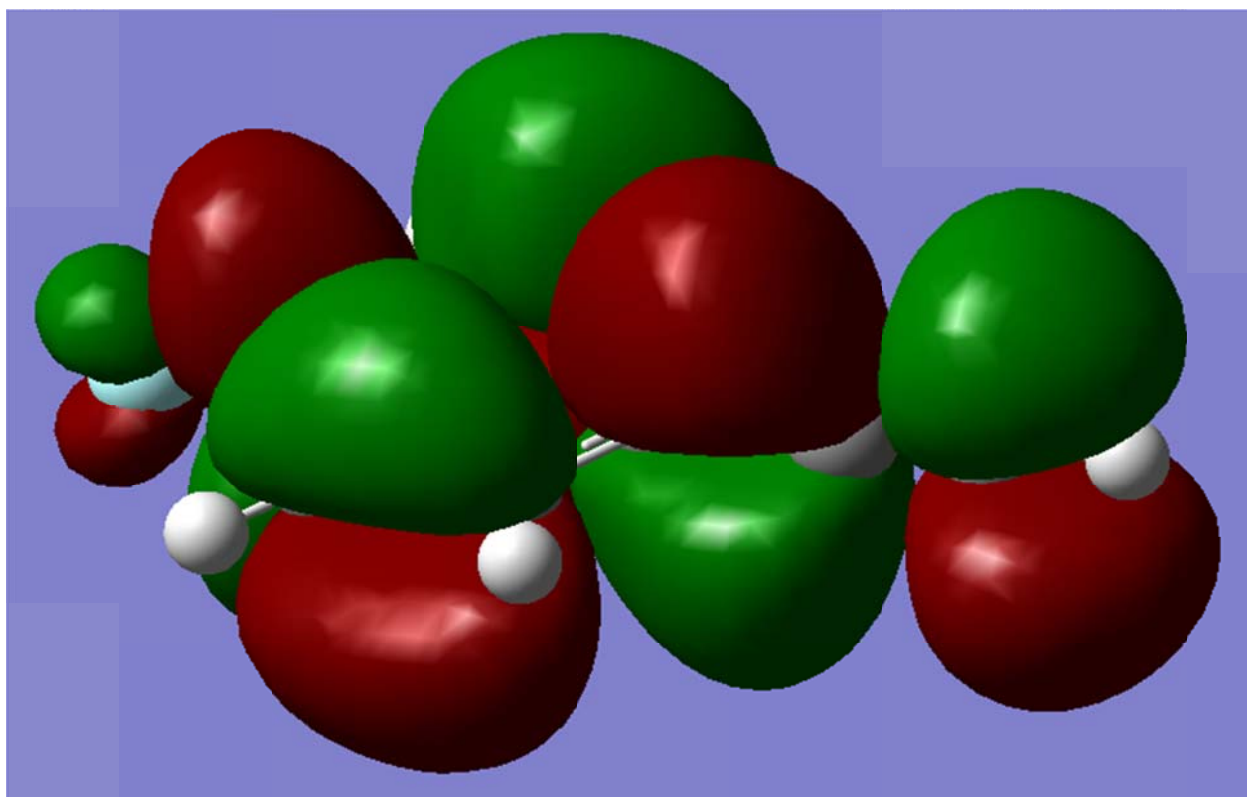
Figure 6: LUMO of 5 at CCSD/cc-pVTZ.
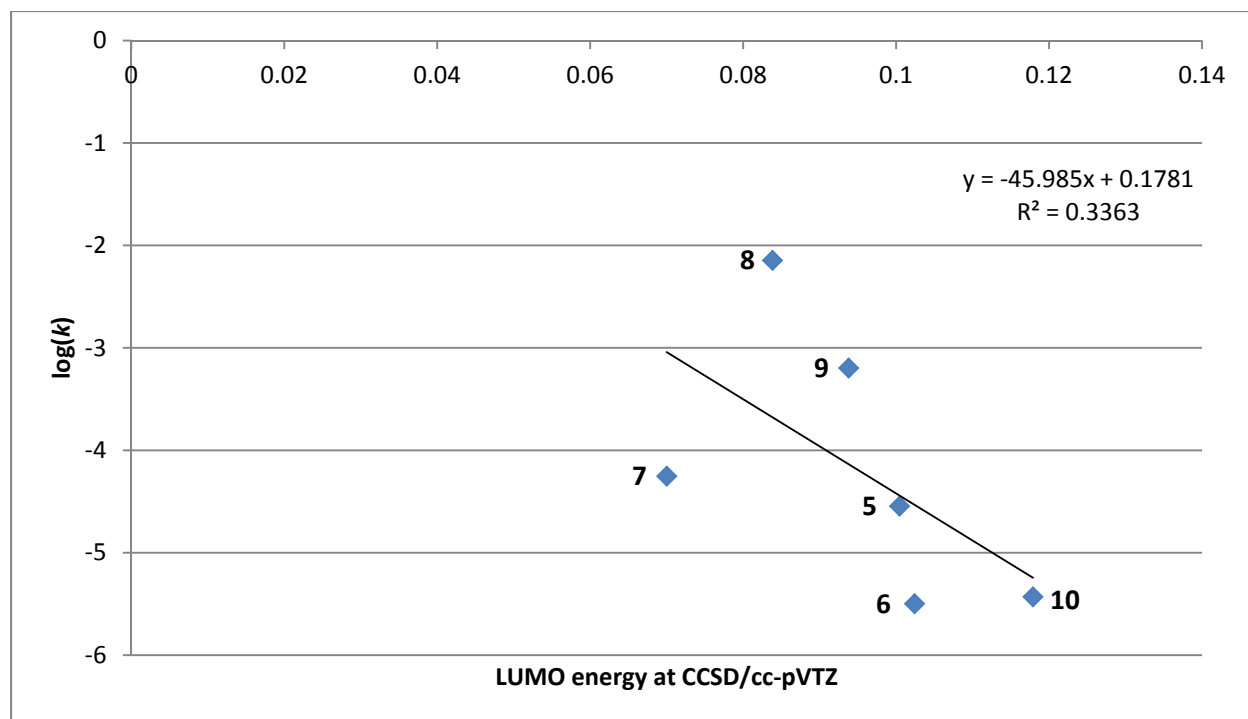
Figure 7: Plot of log(*k*) vs. LUMO energy.

In addition, coupled cluster calculations were performed on **12** in order to attempt to explain the reactivity difference seen between **5** (which favors substitution) and **12** (which favors addition). By inspecting the first few LUMO orbitals, it was hypothesized that because the LUMO of **5** (Figures 5-6) had density on the fluorine bearing carbon, it would allow for substitution to occur. Conversely, the LUMO of **12** (Figure 8) has minimal electron density on the fluorine bearing carbon, and therefore favors addition. It was only the LUMO+1 (Figure 9) that had electron density on the fluorine bearing carbon, however this orbital was significantly higher in energy, which would hypothetically lead to slower reactivity, thus correlating with observed results.
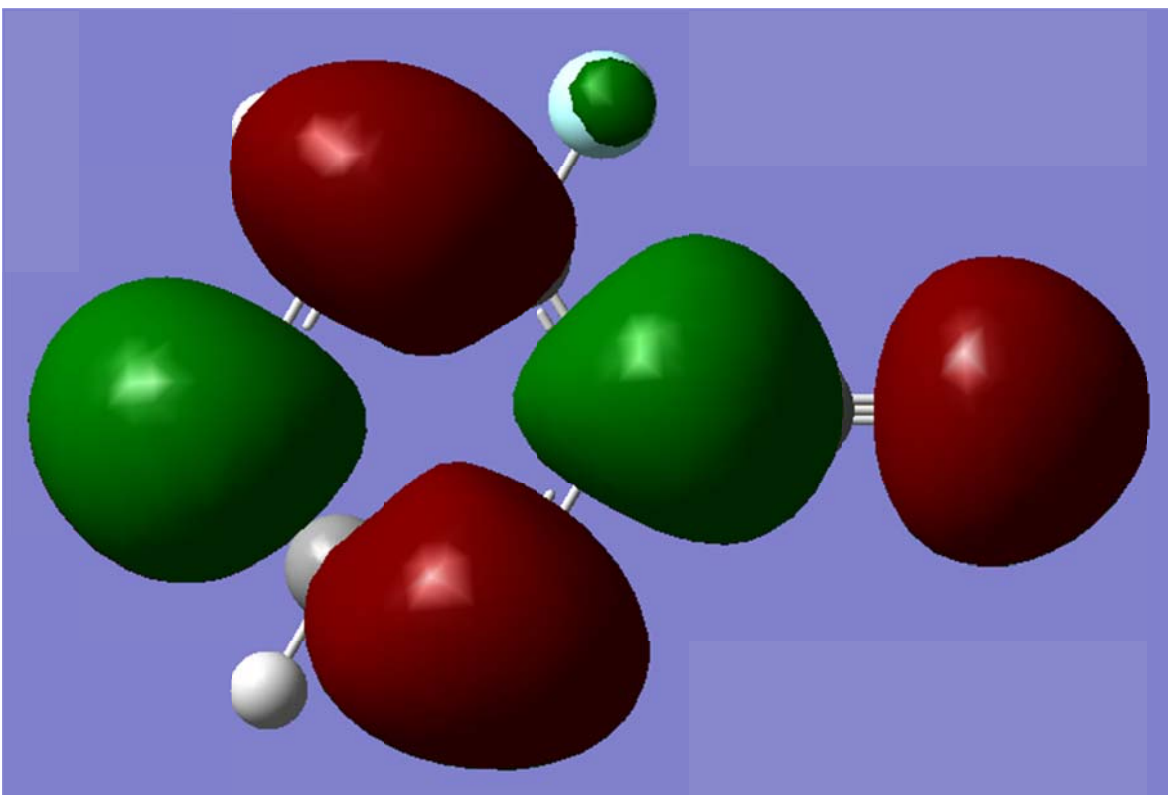
Figure 8: LUMO of 12 at CCSD/cc-pVTZ.
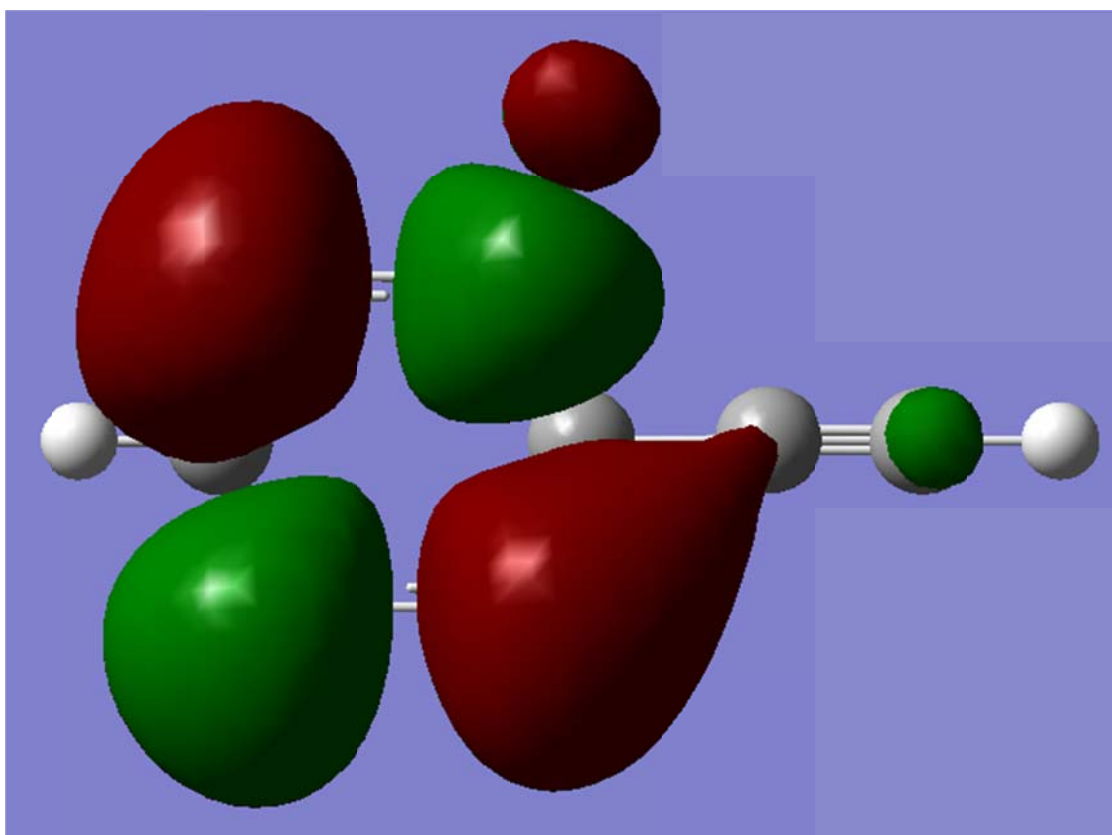
Figure 9: LUMO+1 of 12 at CCSD/cc-pVTZ.

The Arrhenius equation is stated as:

$$k = Ae^{-E_a/RT} \tag{5}$$

Where k is the rate constant, A is the pre-exponential factor, E_a is the activation energy, R is the gas constant, and T is temperature. Using this equation, we can predict, given constant temperature and pre-exponential factor, that the rate constant should be related to the activation energy. Since the rate studies were all run at constant temperature, and the molecules were similar enough that we expect the pre-exponential factor to be the same, this means that this relationship should hold true for the systems under study. To this end, it was hypothesized that computationally calculated activation energies should correlate to the obtained rate data.

In order to calculate activation energy, a model reaction was chosen, and the difference in energy between the reactants and transition states was found. The model chosen was the reaction between the electrophiles and a hydroxide nucleophile since the small size of the hydroxide molecule leads to shorter calculations times. If the accepted reaction coordinate diagram for S_NAr is correct (Figure 10), the transition state should be able to be found using synchronous transit methods (QST2, QST3). However, when these methods were attempted, no transition states were found, leading to minimization to products instead.

It was theorized that although the proposed reaction coordinate (Figure 10) was correct *in situ*, when the reaction was modeled *in silico* in the gas phase with no counter-ion, the reaction coordinate looked quite different due to the instability of the reactants (Figure 11). Because this reaction coordinate was always downhill in energy, it was impossible to find the true transition state because it essentially did not exist in the model. For this reason, another method of modeling had to be found.
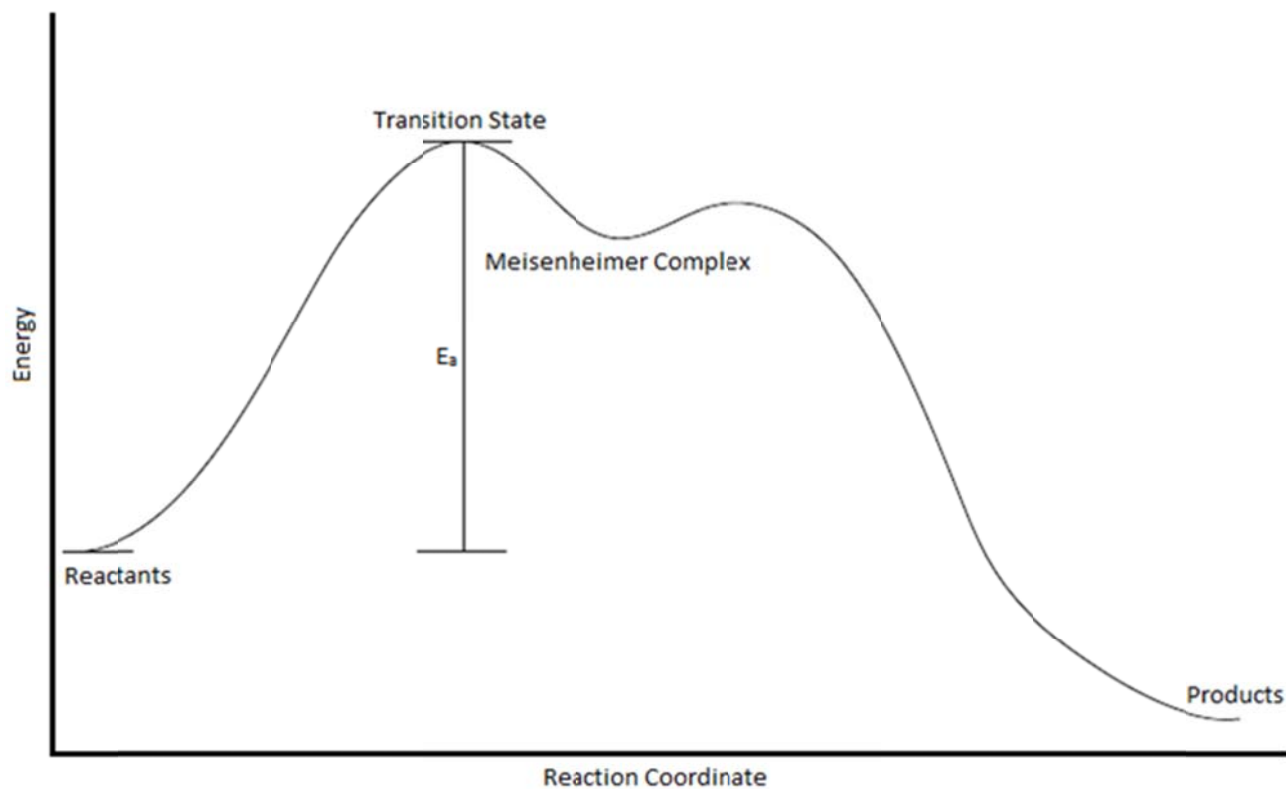
Figure 10: Proposed *in situ* S$_N$Ar reaction coordinate diagram.
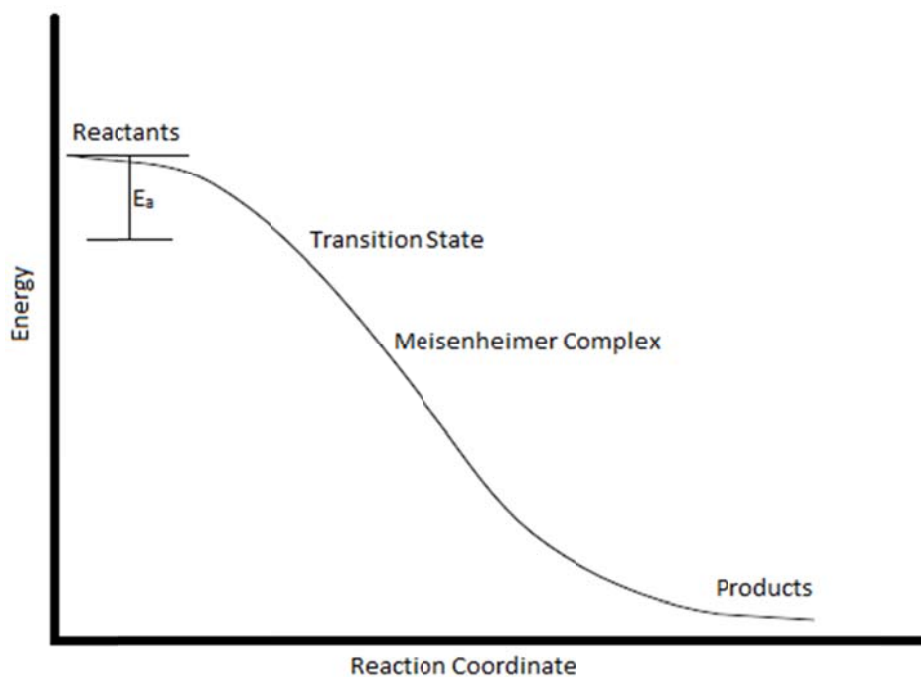
Figure 11: Proposed *in silico* S$_N$Ar reaction coordinate diagram.

In order to find a measure that resembled the activation energy, a point on the reaction coordinate had to be chosen that was thought to mirror the transition state of the system. This

was done by fixing the bond distance between the hydroxide oxygen and the fluorine bearing carbon, then minimizing this pseudo-transition state using density functional theory (B3LYP/6-311+G(d,p)). It was initially hypothesized that fixing the bond distance to resemble a point very early in the reaction coordinate would minimize errors due to the differences in bond distance at the true transition state, but it was found that modeling systems closer to the Meisenheimer complex, which probably more closely resembled the true transition state, actually led to better correlations.

The oxygen-carbon bond distance was fixed at 2.5 Å (early in the reactions coordinate), 2.0 Å, or 1.75 Å (close to the Meisenheimer complex).[b] The difference in energy between these systems and the reactants (all modeled at the same level of theory) was calculated. These values, as predicted by the *in silico* reaction coordinate, are all negative energies, where a larger negative value corresponds to faster reactivity. By calculating the correlation between these energies and experimental rate data, it was found that bond distances of 1.75 Å and 2.0 Å led to the best correlations for this method (Figures 12-13).

Frequency analysis calculations were performed on all DFT minimized pseudo-transition state structures, and all structures did have one imaginary frequency that appeared to correlate to the reaction coordinate. Using these structures, intrinsic reaction coordinate (IRC) calculations were performed. It was found that IRC calculations could only proceed successfully in the forward direction, down the energy gradient. By starting at a long carbon-oxygen bond distance, the proposed *in silico* reaction coordinate was reproduced as hypothesized. Attempts to use several points on the reaction coordinate diagram to find better correlations with rate data were unsuccessful.

---

[b] A 1.5 Å bond distance was also attempted, but led to minimization to products.
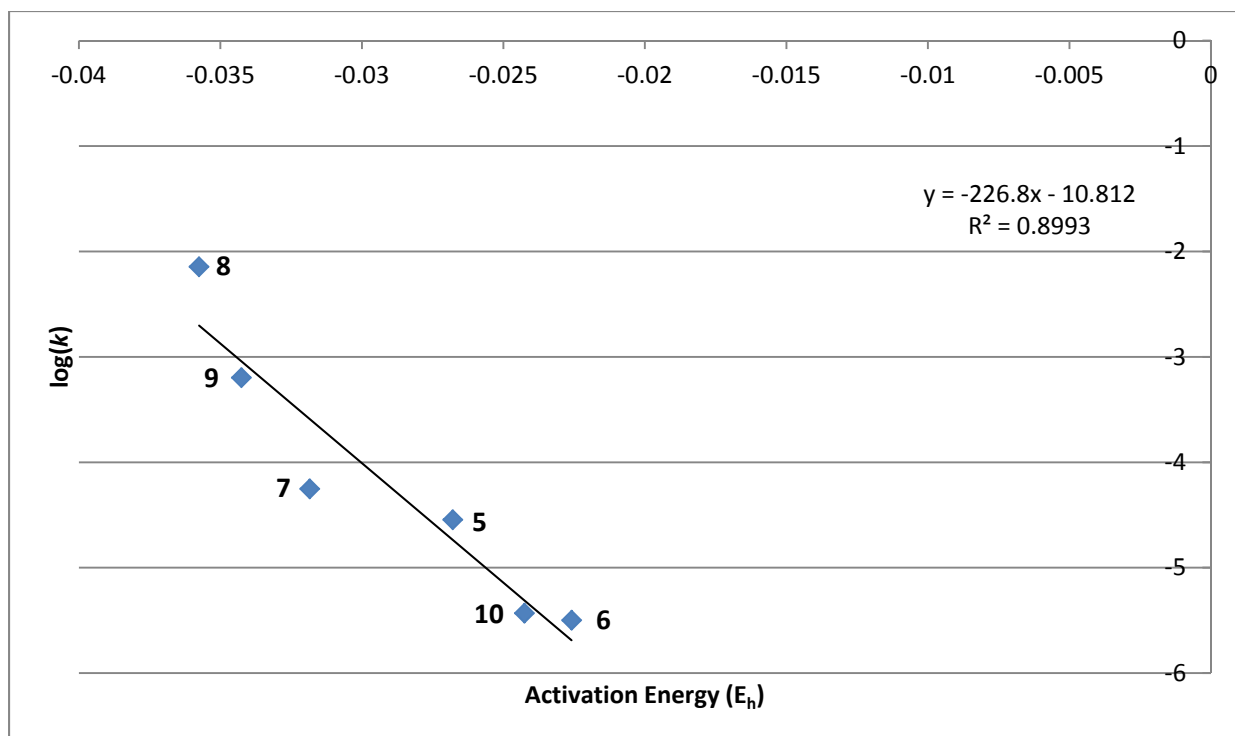
Figure 12: Plot of log(*k*) vs. activation energy using 2.0 Å bond distance modeled at B3LYP/ 6-311+G(d,p).
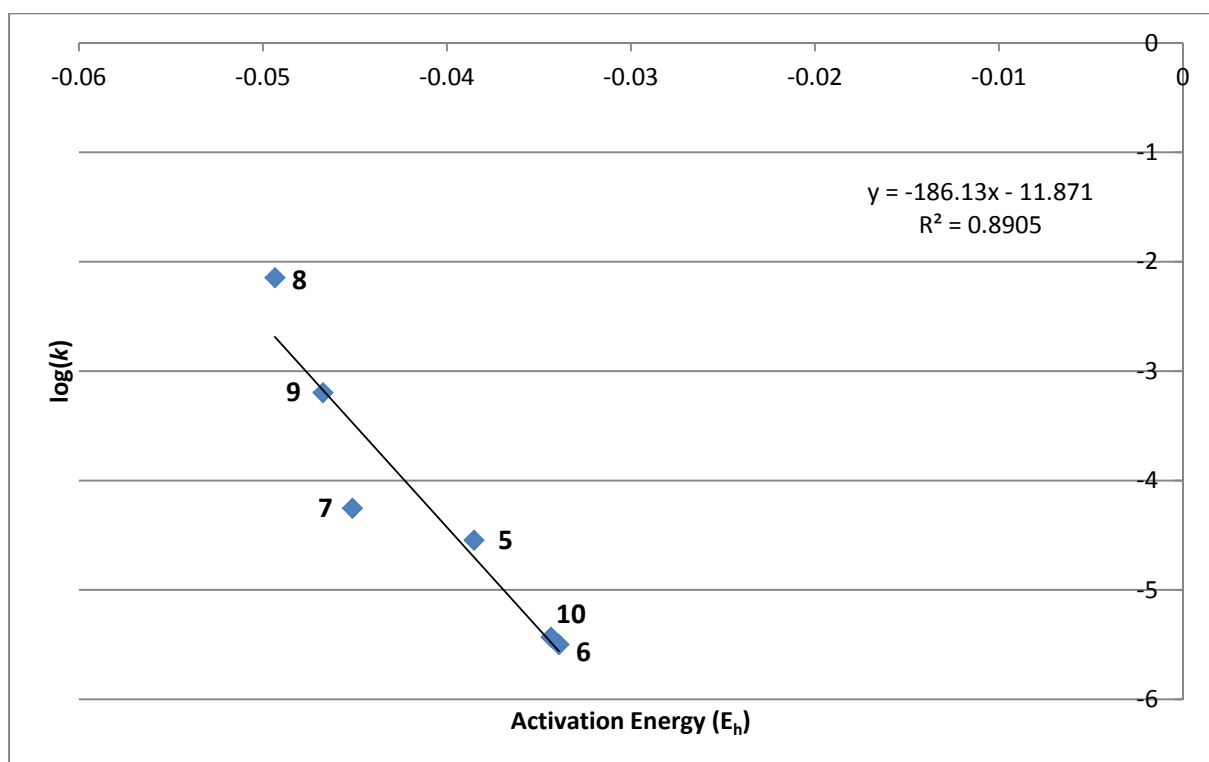
Figure 13: Plot of log(*k*) vs. activation energy using 1.75 Å bond distance modeled at B3LYP/ 6-311+G(d,p).

Using the DFT minimized structures, additional single point energy calculations were performed using various levels of theory in order to measure the effect of calculation type on the correlation. Using the 2.0 Å minimized structures, calculations were performed at AM1 (Figure 14), PM6 (Figure 15), and MP2/6-311+G(d,p) (Figure 16). Using the 1.75 Å minimized structures (general configurations similar to Figure 19), calculations were performed at MP2/6-311+G(d,p) (Figure 17) and MP4(SDTQ)/6-311+G(d,p) (Figure 18). Higher levels of theory generally led to better correlations.
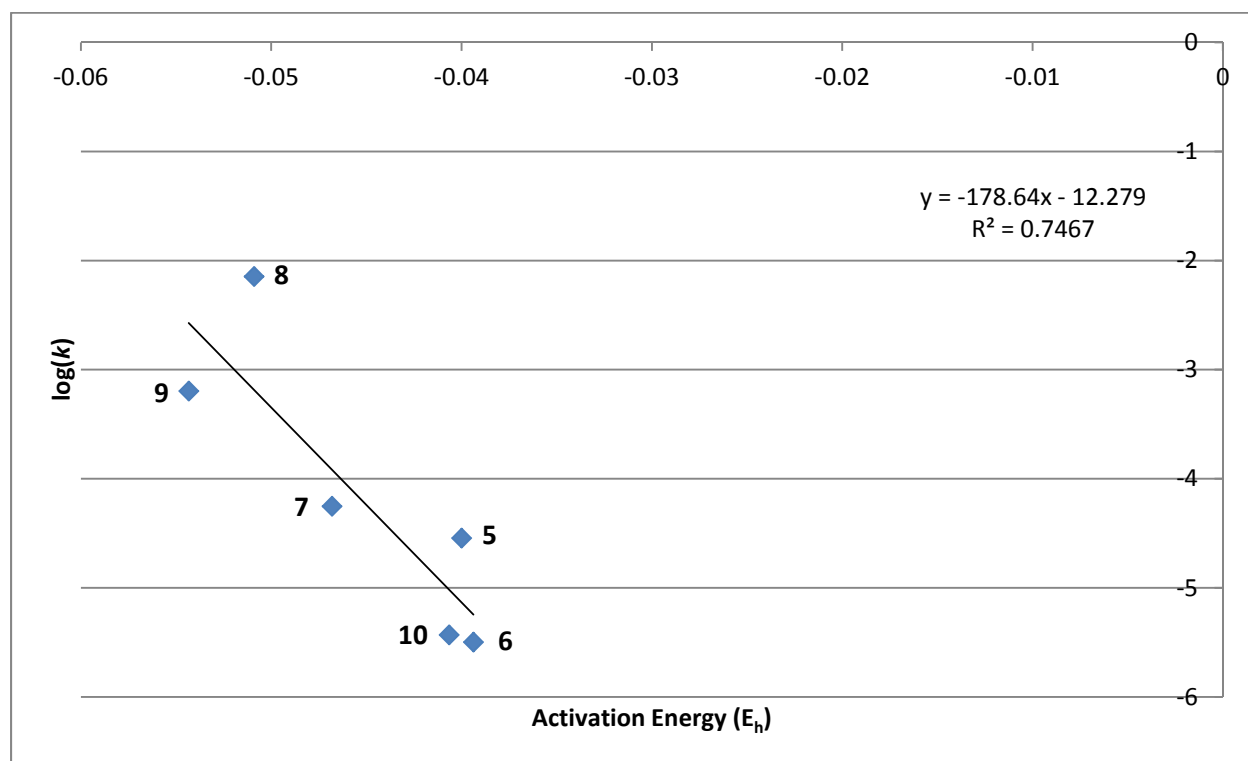
Figure 14: Plot of log(*k*) vs. activation energy using 2.0 Å bond distance modeled at semi-empirical AM1.
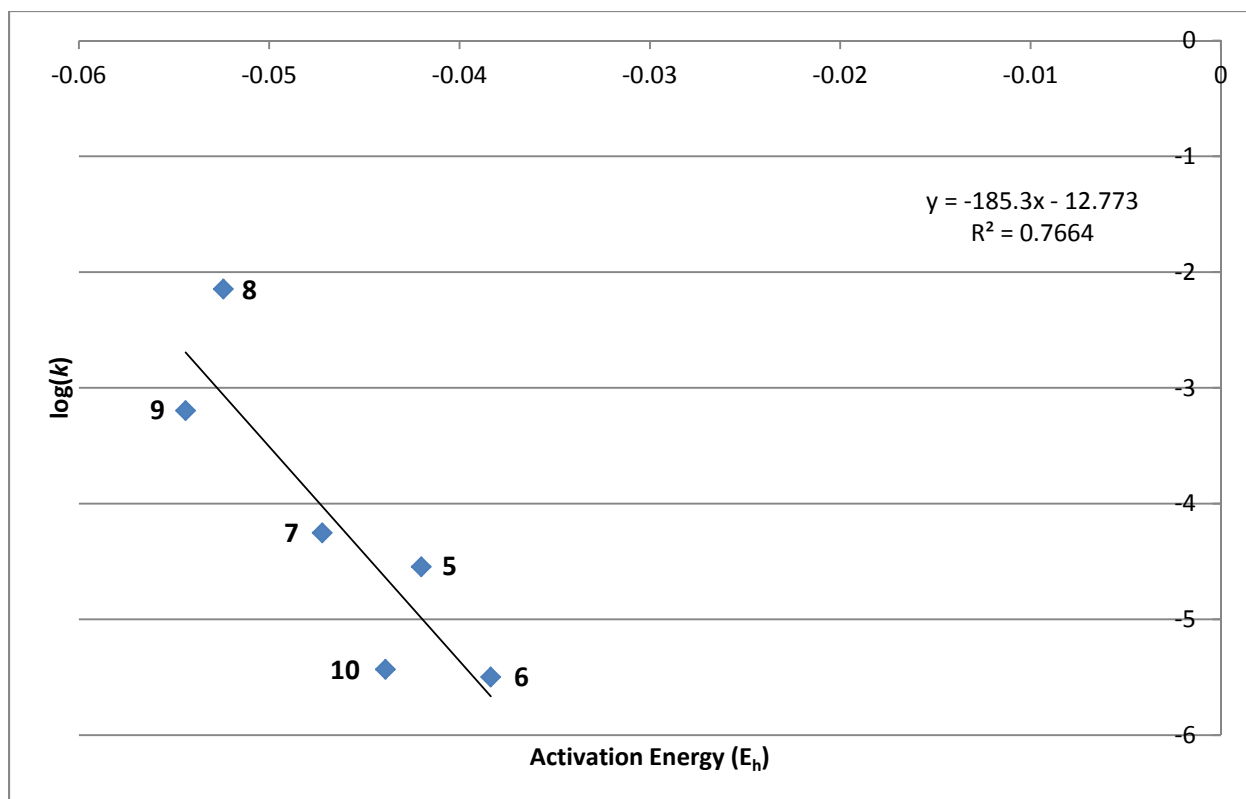
Figure 15: Plot of log(k) vs. activation energy using 2.0 Å bond distance modeled at semi-empirical PM6.
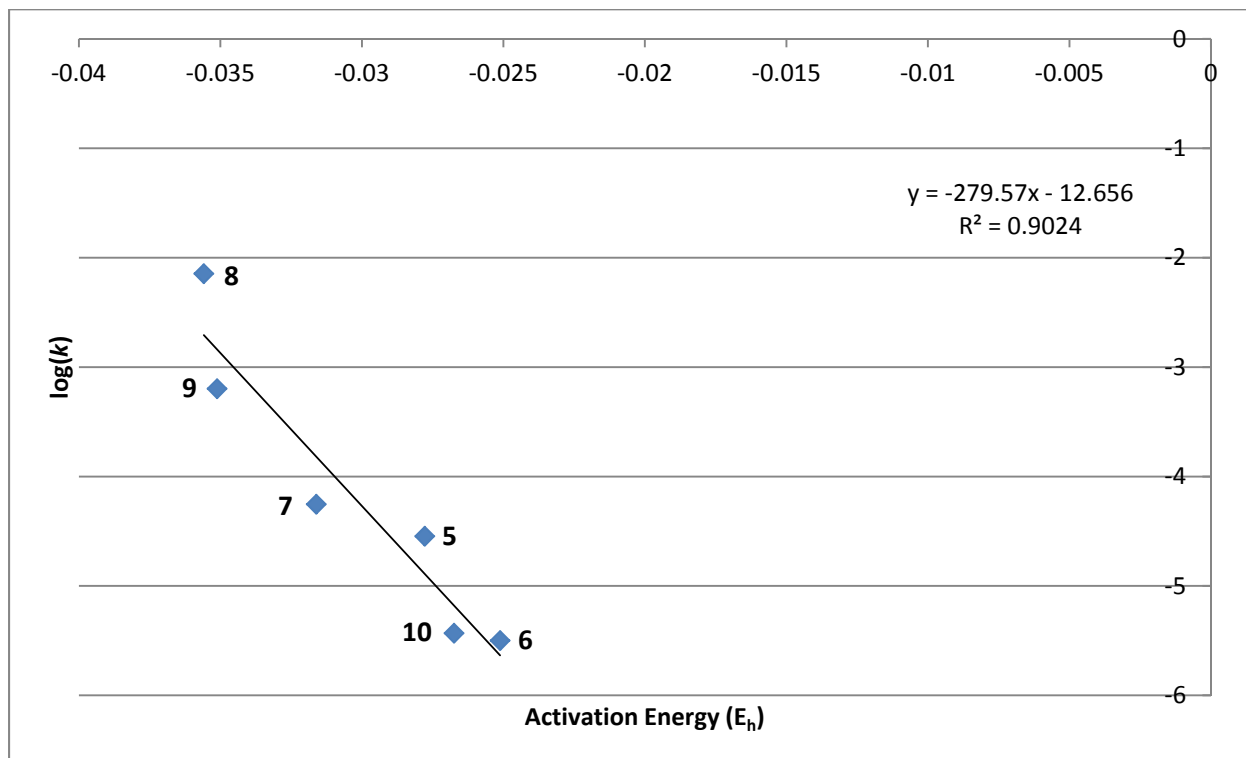
Figure 16: Plot of log(*k*) vs. activation energy using 2.0 Å bond distance modeled at MP2/6-311+G(d,p).
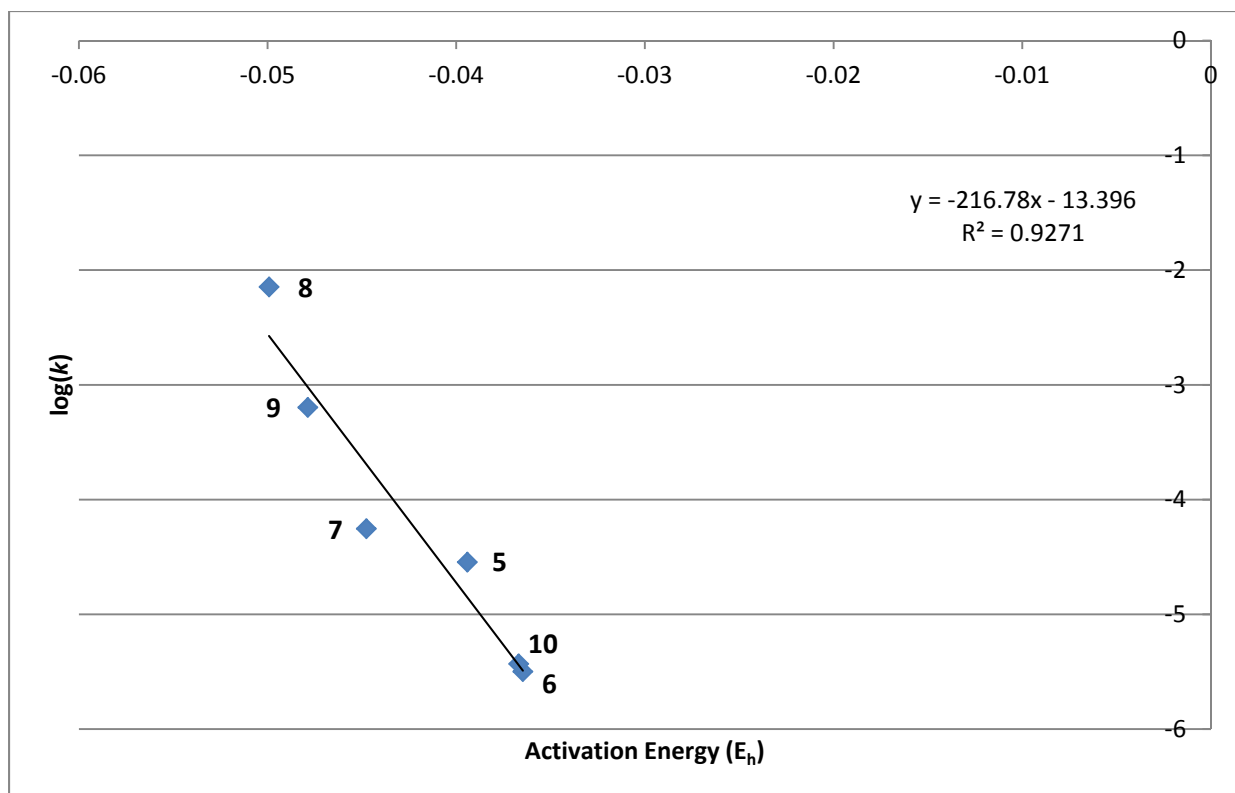
Figure 17: Plot of log(k) vs. activation energy using 1.75 Å bond distance modeled at MP2/ 6-311+G(d,p).
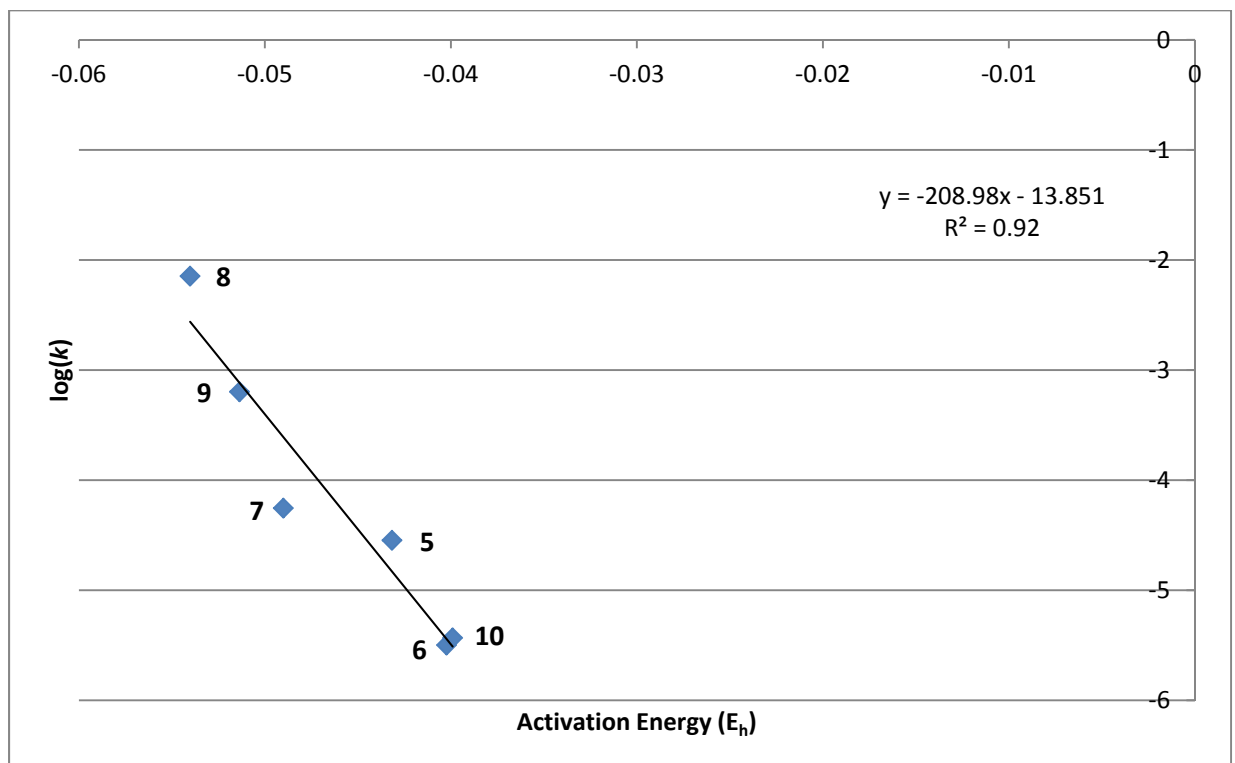
Figure 18: Plot of log(k) vs. activation energy using 1.75 Å bond distance modeled at MP4(SDTQ)/ 6-311+G(d,p).
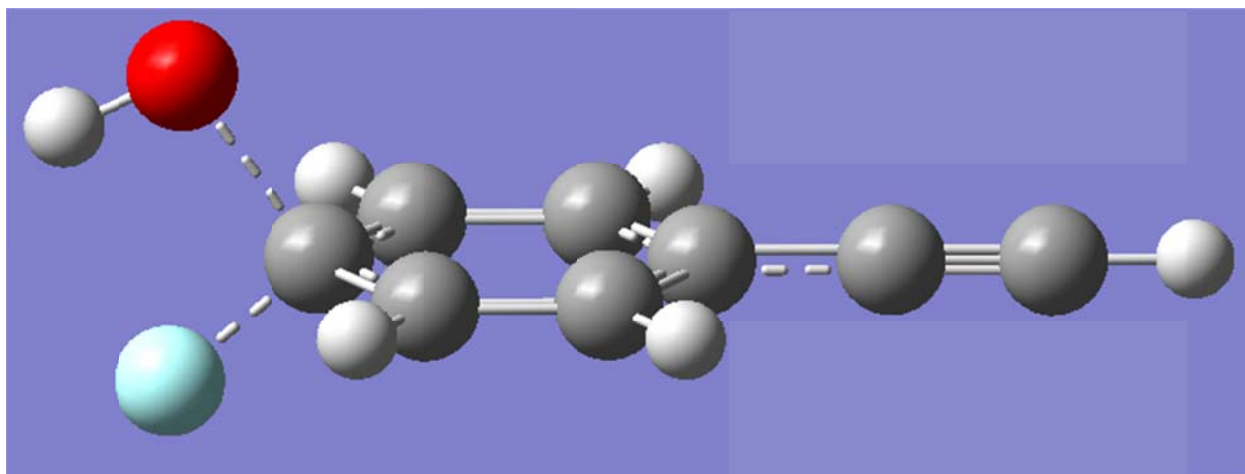
Figure 19: Minimized pseudo-transition state of 4-fluorophenylacetylene with 1.75 Å carbon-oxygen bond distance.

Additional computational calculations were performed in a similar fashion but with the addition of a self-consistent reaction field (SCRF) to model solvation effects. The polarizable continuum model (PCM) using the integral equation formalism variant (IEFPCM) was used with parameters to model DMSO as the solvent, as was the case with the *in situ* reactions. Using this method, synchronous transit-guided quasi-newton (STQN) calculations were performed in order to find the transition states, which did exist *in silico* when a solvation model was used. QST3 was used at HF/3-21+G in order to find an initial transition state structure at a low level of theory, and then the Berny algorithm was used to find the first-order saddle point at B3LYP/6-311+G(d,p). Frequency calculations at the same level of theory verified one imaginary frequency corresponding to the expected reaction coordinate.

IRC calculations were performed on the transition state of phenylacetylene **5**, and it was found that the reaction coordinate could be followed in both directions, and that a saddle point had indeed been found. When analyzed, the reaction coordinate looked as expected, and when followed far enough in the forward direction a potential energy surface minimum was found, which likely corresponded to the Meisenheimer complex. (Figure 20) Attempts to minimize

directly to the Meisenheimer complex were unsuccessful, likely because of the shallow nature of the PES well.

Investigations revealed that two transitions states were possible for the reaction of hydroxide with the electrophiles; one where the hydrogen-oxygen-carbon-fluorine dihedral angle was 0°, and one where it was 180°. Modeling revealed that although both reactions could be followed in both directions using IRC, the 180° dihedral systems led to lower energies, and it was only in this system that the PES minimum previously discussed was found. For these reasons it was determined that the 180° system was a better model and thus it was used for all analysis. (Figure 21)
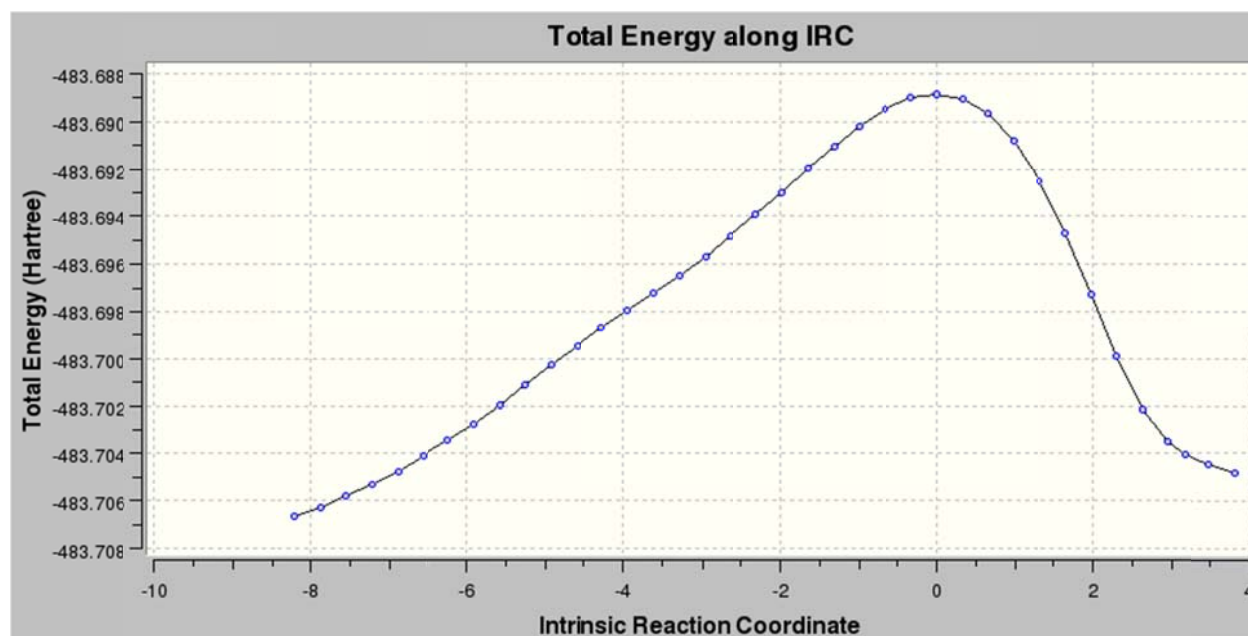
Figure 20: Calculated reaction coordinate diagram for reaction of phenylacetylene 5 with hydroxide using a 180° H-O-C-F dihedral angle.
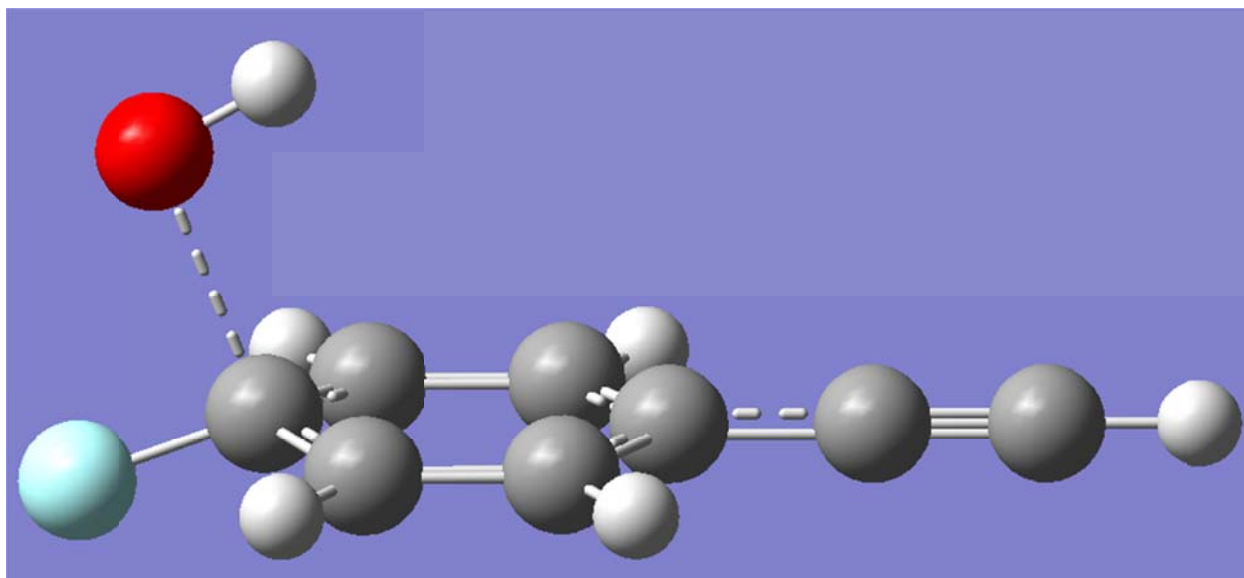
Figure 21: Transition state of 4-fluorophenylacetylene found using the Berny algorithm at B3LYP/6-311+G(d,p).

Transition states were determined for electrophiles **5-10**, and the difference in energy between the transition states and the reactants (all modeled at the same level of theory with a solvation model) was again calculated as previously discussed. (Table 4) The correlation between these activation energies and experimental rate data was found to be far better than the observed correlation when no solvation model was used. (Figure 22). Using the DFT minimized ground state and transition state structures, additional single point energy calculation were performed at MP2/6-311+G(d,p), and the correlation was found. (Figure 23). The DFT correlation was found to be better, which could be because this method was used to generate the transition structures.

The carbon-oxygen bond length in the transition state was also analyzed. (Table 4) These bond lengths, which ranged from ca. 1.97 – 2.14 Å, were longer than originally anticipated and suggested that a 2.0 Å fixed bond length is actually more representative of the transition states than a 1.75 Å fixed bond length. In addition, it was observed that transition state carbon-oxygen

bond length increased with increasing electron withdrawing ability of the EWG, and there was a reasonably high correlation between bond length and experimental rate. (Figure 24)

Table 4: the experimental rate, calculated activation energies, and transition state carbon-oxygen bond length of electrophiles used for rate studies.

Electron Withdrawing Group	log(Rate) (exp.)	E_a (B3LYP)	E_a (MP2)	C-O Bond Length (Å)
Ethynyl (**5**)	-4.545	0.01973542	0.01561956	2.04093
t-Butylethynyl (**6**)	-5.498	0.02240175	0.01716071	2.00268
Phenylethynyl (**7**)	-4.252	0.01974659	0.0153655	2.05286
Acetyl (**8**)	-2.146	0.01554844	0.01274095	2.13595
Trifluoromethyl (**9**)	-3.197	0.01717318	0.01343037	2.07437
Bromide (**10**)	-5.431	0.02243064	0.01742035	1.97657
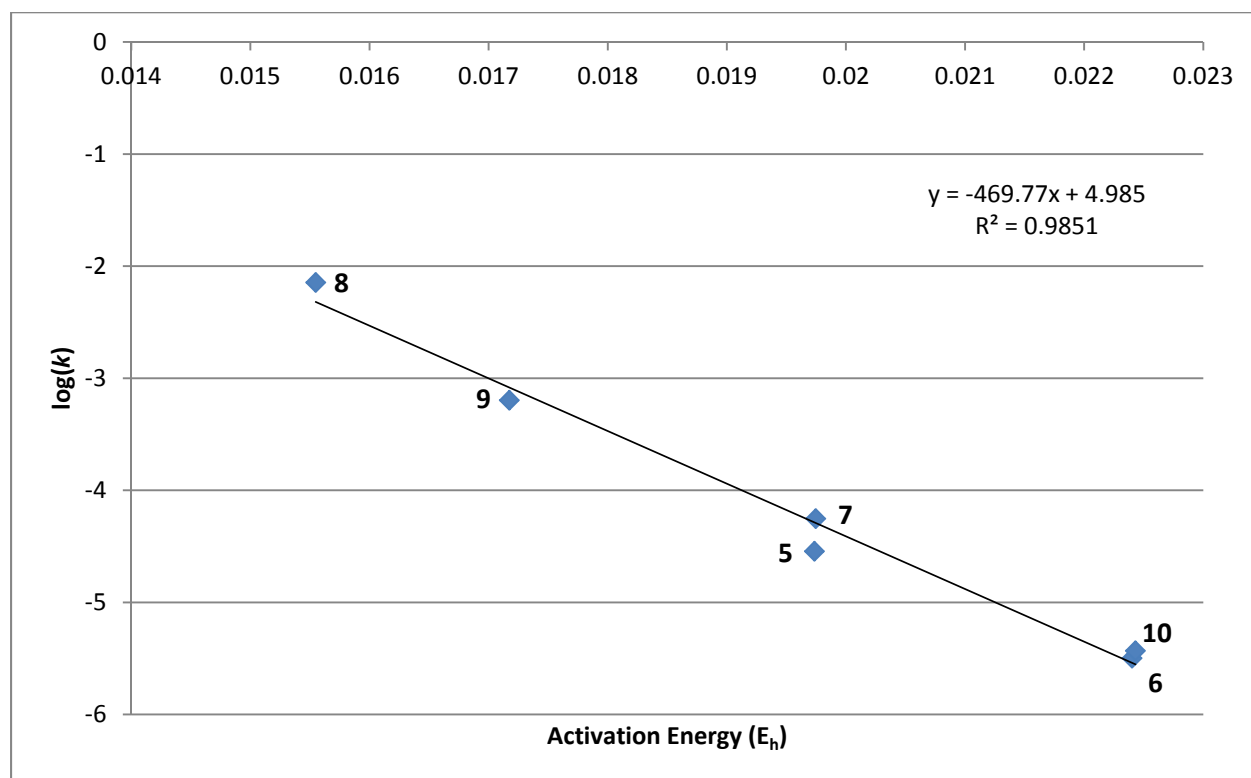
Figure 22: Plot of log(*k*) vs. activation energy using transition state structures modeled at B3LYP/ 6-311+G(d,p).
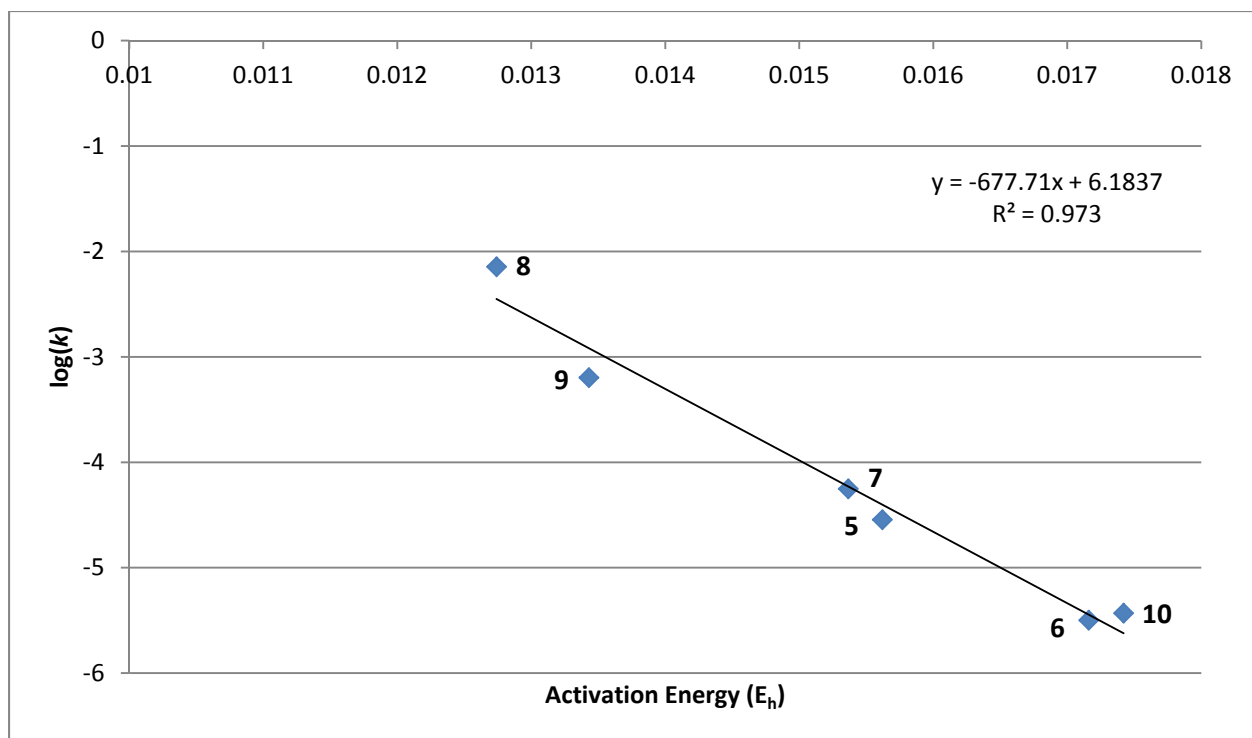
Figure 23: Plot of log(*k*) vs. activation energy using transition state structures modeled at MP2/ 6-311+G(d,p).
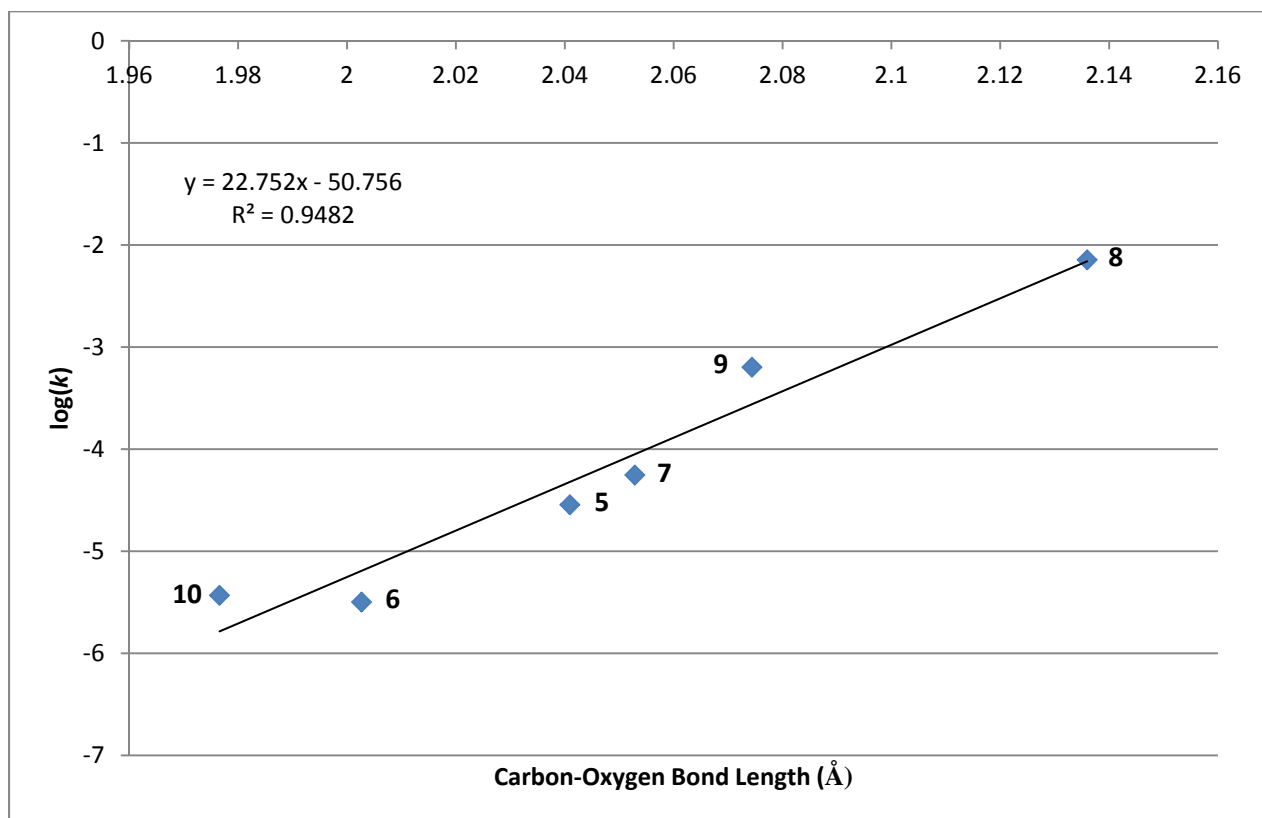
Figure 24: Plot of log(*k*) vs. carbon-oxygen bond length in B3LYP transition states.

Electrophiles **13**-**17** and **26**-**29** were modeled using the transition state method previously described. Using the fit line from the B3LYP transition state calculations, theoretical reaction rates of these electrophiles were determined. Once the rate was calculated, the rate relative to 4-fluorophenylacetylene and the σ_p^- value were found using the experimentally derived data previously discussed. (Section 2.4, Figure 1) Transition state carbon-oxygen bond lengths were also found. (Table 4)
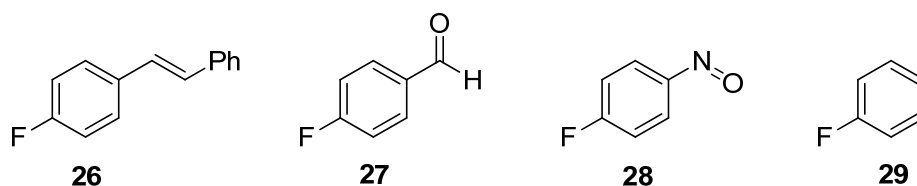
Table 5: The calculated rates, σ_p^- values, and transition state carbon-oxygen bond lengths for several electron withdrawing groups.

Electron Withdrawing Group	Rel. Rate	σ_p^- (calculated)	σ_p^- (literature[14])	C-O Bond Length (Å)
1-Hexynyl (**13**)	0.082	0.22	n/a	1.999
Fluoride (**14**)	0.0015	-0.09	-0.03	1.916
Vinyl (**15**)	0.042	0.17	n/a	1.998
Nitrile (**16**)	1,570	0.98	1.00	2.148
Nitro (**17**)	372,000	1.40	1.27	2.319
(E)-Styryl (**26**)	0.12	0.25	0.13	2.023
Aldehyde (**27**)	2,500	1.01	1.03	2.188
Nitroso (**28**)	3,040,000	1.56	1.63	2.461
Hydrogen (**29**)	0.00056	-0.16	0 (defined)	1.899

It is notable that fluoride and hydrogen EWGs both led to significantly slower calculated rates than acetylene and even bromide. Also notable is the calculated rate for a vinyl EWG, which is comparable to the rates for bromide and *t*-butylethynyl. It is likely only because of competing addition and polymerization processes that this reaction was unsuccessful when attempted *in situ*. As can be seen, the calculated σ_p^- values for nitrile, nitro, aldehyde, and nitroso EWGs are all quite similar to the value reported by Taft,[14] giving additional merit to the

computational methods, and suggesting that this modeling method could even be used to predict new σ_p^- values to a reasonable degree of accuracy.

3. EXPERIMENTAL

3.1 General

All reactions were run under an inert atmosphere of argon and carried out in oven-dried glassware unless otherwise noted. Reagents were used as received from the supplier unless otherwise noted. For flash chromatography, 200–430 mesh silica was used. All NMR spectra were collected on a Varian VNMRS-500 spectrometer. Automatic tuning, shimming, and locking were performed before each spectrum was taken. GC-MS spectra were taken on an Agilent 7890A GC using an Agilent HP5-MS capillary column (30 m × 0.25 mm, 0.25 μm film thickness) with an Agilent 5975C MSD using helium carrier gas. The MS temperature was set at 265 °C, the ionization energy was set at 70 eV, and the mass scan range was 20–400 amu. Microwave reactions were carried out in a Biotage Initiator Microwave Synthesis apparatus.

A "standard acid workup" entails dissolving the reaction solution in ca. 50 mL 1M HCl, then extracting 3x with ca. 30 mL CH_2Cl_2. The organic layers were combined, and washed with ca. 50 mL of a 4:1 mixture of saturated NaCl and 1M HCl. The organic layer was dried over Na_2SO_4, and volume was reduced *in vacuo*.

3.2 Sonogashira Coupling

1-(Trimethylsilylethynyl)-2,6-dichlorobenzene (1): 1-bromo-2,6-dichlorobenzene (218.1 mg, 0.90 mmol), $PdCl_2(PPh_3)_2$ (58.9 mg, 0.08 mmol), and CuI (42.7 mg, 0.22 mmol) were added to a 25 mL test tube with a Schlenk neck inlet. The tube was sealed with a septum, and placed under an argon atmosphere. Distilled, degassed triethylamine (2 mL), followed by trimethylsilylacetylene (1.5 mL, 10 mmol) were added using airfree techniques. The solution was observed to turn black almost immediately upon addition of trimethylsilylacetylene. The

solution was allowed to stir at 65 °C ca. 28 h. A standard acid workup was performed, followed by a petroleum ether (30-60 °C boiling) flash silica column. The solvent was removed *in vacuo*, and the resulting liquid was dried overnight under N_2, yielding a clear oil (115mg, 50% yield). ^{1}H NMR (500 MHz, CDCl$_3$, δ): 7.31 (d, *J* = 8.3 Hz, 2H), 7.14 (t, *J* = 8.1 Hz, 1H), 0.29 (s, 9H); GC-MS (retention time [m/z]): 11.4 min [242.0, 227.0, 128.1, 113.2, 63.0].

1,4-Bis(trimethylsilylethynyl)-2,6-difluorobenzene (2): 1-iodo-2,6-difluoro-4-bromobenzene (503 mg, 1.58 mmol), PdCl$_2$(PPh$_3$)$_2$ (73 mg, 0.10 mmol), and CuI (37 mg, 0.19 mmol) were added to a 25 mL test tube with a Schlenk neck inlet. The tube was sealed with a septum, and placed under an argon atmosphere. Distilled, degassed triethylamine (2.5 mL), followed by trimethylsilylacetylene (3.0 mL, 23 mmol) were added using airfree techniques. The solution was allowed to stir at 70 °C ca. 20 h. A standard acid workup was performed, followed by a hexanes flash silica column. The solvent was removed *in vacuo*, yielding a yellow-white crystalline solid. ^{1}H NMR (500 MHz, CDCl$_3$, δ): 6.97 (d, *J* = 7.4 Hz, 2H), 0.26 (s, 9H), 0.23 (s, 9H); GC-MS (retention time [m/z]): 9.55 min [305.5, 293.0, 291.0, 138.1, 72.8].

1-(1-Hexynyl)-2,6-difluoro-4-bromobenzene (3): 1-iodo-2,6-difluoro-4-bromobenzene (541.0 mg, 1.7 mmol), PdCl$_2$(PPh$_3$)$_2$ (55.9 mg, 0.08 mmol), and CuI (35.1 mg, 0.18 mmol) were added to a 25 mL test tube with a Schlenk neck inlet. The tube was sealed with a septum, and placed under an argon atmosphere. Distilled, degassed triethylamine (2.2 mL), followed by 1-hexyne (0.2 mL, 1.8 mmol) were added using airfree techniques. The solution was allowed to stir at 70 °C ca. 20 h. A standard acid workup was performed, followed by a hexanes flash silica column. The solvent was removed *in vacuo*, yielding product. ^{1}H NMR (500 MHz, CDCl$_3$, δ): 6.88 (d, *J* = 7.8 Hz, 2H), 1.4-2.5 (broad, m, 9H).

1,3-Bis(trimethylsilylethynyl)-4,6-difluorobenzene **(4):** 1,3-dibromo-4,6-difluorobenzene (409.3 mg, 1.5 mmol), PdCl$_2$(PPh$_3$)$_2$ (58.0 mg, 0.08 mmol), and CuI (31.2 mg, 0.16 mmol) were added to a 10 mL round bottom flask. The flask was sealed with a septum, and placed under an argon atmosphere. Distilled, degassed triethylamine (2.2 mL), followed by trimethylsilylacetylene (0.5 mL, 4.2 mmol) were added using airfree techniques. The solution was allowed to stir at 65 °C ca. 18 h. Upon cooling, the solution had turned into a black solid. A standard acid workup was performed, followed by a petroleum ether (30-60 °C boiling) flash silica column. The solvent was removed *in vacuo*, yielding a clear liquid (223 mg, 48% yield). ^{1}H NMR (500 MHz, CDCl$_3$, δ): 7.58 (t, *J* = 7.9 Hz, 1H), 6.81 (t, *J* = 9.0 Hz, 1H), 0.25 (s, 18H).

1,3-Bis(trimethylsilylethynyl)-4,6-difluorobenzene (4): 1,3-dibromo-4,6-difluorobenzene (1.64 g, 6.05 mmol), PdCl$_2$(PPh$_3$)$_2$ (221.6 mg, 0.32 mmol), and CuI (114.8 mg, 0.60 mmol) were added to a 25 mL round bottom flask. The flask was sealed with a septum, and placed under an argon atmosphere. Distilled, degassed triethylamine (9.0 mL), followed by trimethylsilylacetylene (1.75 mL, 13.5 mmol) were added using airfree techniques. The solution was allowed to stir at 65 °C ca. 18 h. Upon cooling, the solution had turned into a black solid. A standard acid workup was performed, followed by a hexanes flash silica column. The solvent was removed *in vacuo*, yielding a clear liquid (1.3 g, 70% yield). ^{1}H NMR (500 MHz, CDCl$_3$, δ): 7.58 (t, *J* = 7.9 Hz, 1H), 6.81 (t, *J* = 9.0 Hz, 1H), 0.25 (s, 18H).

3.3 S$_N$Ar Rate Studies

SnAr rate studies were performed by follow the below scheme as closely as possible in order to minimize experimental error, and keep any systematic error constant.

To a 2.0-5.0 mL Biotage microwave test tube was added p-cresol (1.5-1.7 mmol) and potassium *tert*-butoxide (1.6-1.8 mmol), measured by mass. A small Biotage magnetic stir bar was added, and the tube was sealed using a Biotage cap with a resealable septum. The tube was flushed with argon gas using a positive pressure house argon system, and dry dimethylsulfoxide with ~280mM 1,3-dimethyl-2-imidazolidone (DMSO+DMI, 2.7 mL) was added via Schlenk techniques using a 3.0 mL plastic Luer-Slip syringe with an 18 gauge 9 cm stainless steel needle. This solution was heated to 85 °C while stirring, until the solution was homogeneous. The argon line was removed, and the electrophile (1.0 mmol) was added using a 250 µL glass Luer-Slip syringe with a 19 gauge 9 cm stainless steel needle.

In cases where the electrophile was not a liquid, only 1.7 mL DMSO+DMI was added in the previous step. The solid electrophile was weighed by mass into a 5 mL pear-shaped round bottom flask, a small magnetic stir bar was added, and the flask was fitted with a standard septa and put under positive pressure argon. To this flask was added DMSO+DMI (1.0 mL) via Schlenk techniques, and the solution was heated to 85 °C while stirring, until homogeneous. The solution was transferred into the Biotage microwave test tube via a 3.0 mL plastic Luer-Slip syringe fitted with an 18 gauge 9 cm stainless steel needle. In this case the argon line was not removed from the Biotage test tube until the solutions were mixed to avoid excessive positive pressure buildup, which caused problems during aliquot removal procedures.

Upon addition of the electrophile, a timer was started, and immediately (within 5-10 seconds) an aliquot was taken (see below). Reactions were run on timescales ranging from 30 minutes to 200 hours. Between 8 and 10 aliquots were taken for each reaction, usually approximately doubling the time interval between each aliquot.

Aliquots were taken by fitting a 1.0 mL plastic Luer-Slip syringe with an 18 gauge 9 cm stainless steel needle, and inserting the needle through the resealable septum into the reaction solution. The syringe was drawn up until the liquid level reached 0.05 – 0.08 mL, and the syringe was then removed and the liquid released into 1M HCl (~1.5 mL) contained in a small vial with a PTFE lined screw-cap. The resulting mixture was shaken to ensure complete quenching of reaction, and CDCl3 (99% atom-D, ~0.5 – 0.8 mL) was added and the mixture was shaken again, forming a biphasic mixture upon standing. The bottom layer of this mixture was removed using a glass Pasteur pipette, and put directly into an NMR sample tube. Additional CDCl3 was added to the tube if necessary.

NMR spectra were taken with a spectral width of -1 to 11 ppm, using a 10 second relaxation delay and 64 scans. All other settings were left at their default values. In most cases, spectra were analyzed by integrating the peaks in the aromatic region with the lowest and highest chemical shifts, which corresponded to unreacted p-cresol and the electrophile respectively. The peaks corresponding to the two types of protons on 1,3-dimethyl-2-imidazolidone (DMI) at 2.78 and 3.28 were also integrated.

Concentrations of electrophile and nucleophile were determined according to equations:

$$[E] = \left(\frac{\frac{E_{int}}{2}}{\frac{\frac{Std_{int1}}{4} + \frac{Std_{int2}}{6}}{2}} \right) * [DMI] \tag{6}$$

$$[Nu] = \left(\frac{\frac{Nu_{int}}{2}}{\frac{\frac{Std_{int1}}{4} + \frac{Std_{int2}}{6}}{2}} \right) * [DMI] \qquad (7)$$

Where E_{int} is the integration of the electrophile peak, Nu_{int} is the integration of the nucleophile peak, Std_{int1} is the integration of the DMI peak at 3.28, Std_{int2} is the integration of the DMI peak at 2.78, and *[DMI]* is the concentration of DMI in the reaction solution.

In cases where the highest chemical shift peak was obscured (phenylethynyl and tert-butylethynyl EWGs), one of the non-obscured peaks that corresponded to a pair of hydrogens on the substitution product was integrated. Initial concentration of electrophile was found using the method previously stated, and subsequent concentrations were found by subtracting the concentration of product from the initial electrophile concentration, which is sound assuming no side products are being formed.

Once electrophile and nucleophile concentrations were determined, the time-dependent data was fit to equations 2 and 3 using non-linear least squares curve fitting. This was done by finding the sum of the squares of the difference between the experimental concentrations and the calculated concentrations, and minimizing this sum by varying *k* (the rate constant) using the solver add-in for Microsoft Excel. Once the best value for *k* was found, the standard deviation of *k* was found using the SolverAid macro developed by Robert de Levie.[19]

Average values of *k* were found by taking the arithmetic mean of all values derived from electrophile and nucleophile fits for each EWG. Between 2 and 4 experiments were conducted for each group. Standard deviations were found by taking the standard deviation of the same average values. The standard deviation of *k* values between experiments was generally larger than the standard deviation in the fit (ca. 5-10% vs. ca. 20-30%), but despite this it was

determined that neither source of error could be ignored. Because of this fact along with the small size of our data set, we determined we would be unable to construct an accurate confidence interval for k values, and thus in turn σ values. However, because the σ values are a log transform of k, the error would still likely be quite small.

1-Ethynyl-4-(p-tolyloxy)benzene (reaction of 5 and 11): ^{1}H NMR (500 MHz, CDCl$_3$, δ): 7.41 (d, J = 8.6 Hz, 2H), 7.14 (d, J = 8.6 Hz, 2H), 6.91 (d, J = 8.6 Hz, 2H), 6.88 (d, J = 8.6 Hz), 3.03 (s, 1H, acetylene H), 2.35 (s, 3H, methyl H); GC-MS (retention time [m/z]): 15.17 min [208.2 (100%), 178.1 (10.2%), 165.1 (14.7%), 91.1 (25.1%)].

1-(3,3-Dimethylbut-1-yn-1-yl)-4-(p-tolyloxy)benzene (reaction of 6 and 11): ^{1}H NMR (500 MHz, CDCl$_3$, δ): 7.31 (d, J = 8.8 Hz, 2H), 7.12 (d, J = 8.6 Hz, 2H), 6.88 (d, J = 8.6 Hz, 2H), 6.86 (d, J = 8.8 Hz, 2H), 2.34 (s, 3H, methyl H), 1.32 (s, 9H, t-Bu H).

1-Methyl-4-(4-(phenylethynyl)phenoxy)benzene (reaction of 7 and 11): ^{1}H NMR (500 MHz, CDCl$_3$, δ): 7.49 (m, 2H), 7.45 (d, J = 8.8 Hz, 2H), 7.32 (m, 3H), 7.15 (d, J = 8.4 Hz, 2H), 6.93 (d, J = 8.6 Hz, 2H), 6.92 (d, J = 8.8 Hz, 2H), 2.36 (s, 3H, methyl H).

1-(4-(*p*-Tolyloxy)phenyl)ethanone (reaction of 8 and 11): ^{1}H NMR (500 MHz, CDCl$_3$, δ): 7.90 (d, J = 8.9 Hz, 2H), 7.17 (d, J = 8.5 Hz, 2H), 6.95 (d, J = 8.9 Hz, 2H), 6.94 (d, J = 8.4 Hz, 2H), 2.57 (s, 3H, ketone methyl H), 2.37 (s, 3H, *p*-cresol methyl H).

1-Methyl-4-(4-(trifluoromethyl)phenoxy)benzene (reaction of 9 and 11): ^{1}H NMR (500 MHz, CDCl$_3$, δ): 7.53 (d, J = 8.8 Hz, 2H), 7.17 (d, J = 8.6 Hz, 2H), 7.00 (d, J = 8.9 Hz, 2H), 6.94 (d, J = 8.2 Hz, 2H), 2.37 (s, 3H, methyl H).

1-Bromo-4-(*p*-tolyloxy)benzene (reaction of 10 and 11): ^{1}H NMR (500 MHz, CDCl$_3$, δ): 7.38 (d, J = 8.9 Hz, 2H), 7.13 (d, J = 8.5 Hz, 2H), 6.89 (d, J = 8.5 Hz, 2H), 6.83 (d, J = 8.9 Hz, 2H), 2.34 (s, 3H, methyl H).

3.4 S$_N$Ar with other *ortho* and *para*, and di-substituted fluorobenzenes

Reactions of 1-ethynyl-2-fluorobenzene (12) with *p*-cresol (11):

In DMSO: 1-ethynyl-2-fluorobenzene (29.1 mg, 0.24 mmol), *p*-cresol (38.0 mg, 0.35 mmol), and Cs$_2$CO$_3$ (251.1 mg, 0.77 mmol) were added to a round bottom flask, which was sealed with a septum and put under an argon atmosphere. Dry DMSO (0.85 mL) was added via syringe using airfree techniques. The reaction was allowed to stir ca. 18 h at 125 °C. A standard acid workup was performed, and the product was dried under positive pressure, yielding **18**-**21** in a 4.7**:**6.4**:**2.4**:**1 ratio by GC/MS.

In DMSO-d6: 1-ethynyl-2-fluorobenzene (38.9 mg, 0.32 mmol), *p*-cresol (45.0 mg, 0.42 mmol), and Cs$_2$CO$_3$ (285.6 mg, 0.88 mmol) were added to a round bottom flask, which was sealed with a septum and put under an argon atmosphere. Dry DMSO-d6 (0.85 mL) was added via syringe. The reaction was allowed to stir ca. 48 h at temperatures ranging from 40-130 °C. A standard acid workup was performed, and the product was dried *in vacuo* ca. 18 h, yielding **18**-**21** deuterated in all label proton positions, a brown wet solid, in unknown ratio.

In DMF: 1-ethynyl-2-fluorobenzene (30.5 mg, 0.25 mmol), *p*-cresol (33.0 mg, 0.31 mmol), and Cs$_2$CO$_3$ (256.2 mg, 0.79 mmol) were added to a round bottom flask, which was sealed with a septum and put under an argon atmosphere. Dry DMF (0.85 mL) was added via syringe using airfree techniques. The reaction was allowed to stir ca. 18 h at 125 °C. A standard acid workup was performed, and the product was dried under positive pressure, yielding **18**-**21** in a ca. 5**:**6**:**2.5**:**1 ratio by GC/MS.

In DMSO with CsF: 1-ethynyl-2-fluorobenzene (29.7 mg, 0.23 mmol), *p*-cresol (30.6 mg, 0.28 mmol), and CsF (164.4 mg, 1.08 mmol) were added to a round bottom flask, which was sealed with a septum and put under an argon atmosphere. Dry DMSO (0.85 mL) was added via

syringe using airfree techniques. The reaction was allowed to stir ca. 18 h at 125 °C. A standard acid workup was performed, and the product was dried under positive pressure, yielding **18-21** in a ca. 5**:**6**:**2.5**:**1 ratio by GC/MS.

Reaction of 1-(1-hexynyl)-4-fluorobenzene (13) with *p*-cresol (11): 1-(1-hexynyl)-4-fluorobenzene (175 µL, 1.00 mmol), *p*-cresol (172.8 mg, 1.60 mmol), and *t*-BuOK (191.1 mg, 1.70 mmol) were added to a 2.0-5.0 mL Biotage microwave tube, which was sealed and put under an argon atmosphere. Dry DMSO (2.7 mL) was added via syringe, and the solution was allowed to stir ca. 68h at 85 °C. A large number of addition products were observed by ^{1}H NMR.

Reaction of 1,4-difluorobenzene (14) with *p*-cresol (11): 1,4-difluorobenzene (97 µL, 1.00 mmol), *p*-cresol (114 µL, 1.09 mmol), and Cs_2CO_3 (1.4 g, 4.3 mmol) were added to a 2.0-5.0 mL Biotage microwave tube, which was sealed and put under an argon atmosphere. Dry DMSO (2.7 mL) was added via syringe, and the solution was allowed to stir ca. 24h at 130 °C. No reaction was seen as observed by ^{1}H NMR.

Reaction of 1-fluoro-4-vinylbenzene (15) with *p*-cresol (11): 1-fluoro-4-vinylbenzene (105 µL, 1.15 mmol), *p*-cresol (124.0 mg, 1.15 mmol), and Cs_2CO_3 (1.2 g, 3.7 mmol) were added to a 2.0-5.0 mL Biotage microwave tube, which was sealed and put under an argon atmosphere. Dry DMSO (2.7 mL) was added via syringe, and the solution was allowed to stir ca. 24h at 130 °C. No substitution was seen via ^{1}H NMR, with probable polymer formation of 1-fluoro-4-vinylbenzene observed.

Reaction of 4-fluorobenzonitrile (16) with *p*-cresol (11): 4-fluorobenzonitrile (124.6 µL, 1.0 mmol), *p*-cresol (164.8 mg, 1.52 mmol), and t-BuOK (173.5 mg, 1.55 mmol) were added to a 2.0-5.0 mL Biotage microwave tube, which was sealed and put under an argon atmosphere. Dry DMSO+DMI (2.7 mL) was added via syringe, and the solution was allowed to stir for 30

minutes at 30 °C, with 10 aliquots being taken over the course of reaction using the method outlined above. Substitution was observed to proceed over the time period via ^{1}H NMR, with a half-life of ca. 20 minutes and a k value of ca. 0.001 L·mol^{-1}·s^{-1}.

Reaction of 1-fluoro-4-nitrobenzene (17) with _p_-cresol (11): 1-fluoro-4-nitrobenzene (106 µL, 1.0 mmol), _p_-cresol (167.6 mg, 1.55 mmol), and t-BuOK (184.6 mg, 1.65 mmol) were added to a 2.0-5.0 mL Biotage microwave tube, which was sealed and put under an argon atmosphere. Dry DMSO+DMI (2.7 mL) was added via syringe, and the solution was allowed to stir ca. 5 seconds at 30 °C. Complete substitution was observed via ^{1}H NMR after ca. 5 seconds.

3.6 S$_N$Ar with other nucleophiles

Reaction of 4-fluorophenylacetylene (5) with hexylamine: 4-fluorophenylacetylene (96.4 mg, 0.80 mmol), hexylamine (110 µL, 0.85 mmol), and Cs$_2$CO$_3$ (0.85 g, 2.6 mmol) were added to a 2.0-5.0 mL Biotage microwave tube, which was sealed and put under an argon atmosphere. Dry DMSO (3.0 mL) was added via syringe, and the solution was heated in a microwave for 4h at 175 °C. A large variety of products were observed via ^{1}H NMR.

Reaction of 4-fluorobenzotrifluoride (9) with hexylamine: 4-fluorobenzotrifluoride (124.3 mg, 0.76 mmol), hexylamine (100 µL, 0.80 mmol), and diisopropylethylamine (150 µL, 0.85 mmol) were added to a 2.0-5.0 mL Biotage microwave tube, which was sealed and put under an argon atmosphere. Dry DMSO (2.2 mL) was added via syringe, and the solution was heated in a microwave for 2h at 160 °C. The substitution product was observed via ^{1}H NMR in ca. 90% conversion.

Reaction of 4-fluoroacetophenone (8) with methylamine: 4-fluoroacetophenone (126.0 mg, 0.91 mmol), methylamine (33% solution in ethanol) (100 µL, 0.78 mmol), and

diisopropylethylamine (200 µL, 1.14 mmol) were added to a 2.0-5.0 mL Biotage microwave tube, which was sealed and put under an argon atmosphere. Dry DMSO (2.4 mL) was added via syringe, and the solution was heated in a microwave for 10h at 140 °C. The substitution product was observed via ^{1}H NMR in ca. 55% conversion.

Reaction of 4-fluoroacetophenone (8) with methylamine hydrochloride: 4-fluoroacetophenone (109.0 mg, 0.79 mmol), methylamine hydrochloride (70 mg, 1.03 mmol), and diisopropylethylamine (400 µL, 2.28 mmol) were added to a 2.0-5.0 mL Biotage microwave tube, which was sealed and put under an argon atmosphere. Dry NMP (2.2 mL) was added via syringe, and the solution was heated in a microwave for 16h at 140 °C. The substitution product was observed via ^{1}H NMR in ca. 45% conversion.

Reaction of 4-fluoroacetophenone (8) with methylamine hydrochloride: 4-fluoroacetophenone (138.0 mg, 1.0 mmol), methylamine hydrochloride (73.2 mg, 1.08 mmol), and diisopropylethylamine (450 µL, 2.85 mmol) were added to a 2.0-5.0 mL Biotage microwave tube, which was sealed and put under an argon atmosphere. Dry DMSO (2.8 mL) was added via syringe, and the solution was heated in a microwave for 12h at 140 °C. The substitution product was observed via ^{1}H NMR.

Reaction of 4-fluorophenylacetylene (5) with methylamine: 4-fluorophenylacetylene (89.5 mg, 0.75 mmol), methylamine (33% solution in ethanol) (95 µL, 0.74 mmol), and diisopropylethylamine (175 µL, 1.0 mmol) were added to a 2.0-5.0 mL Biotage microwave tube, which was sealed and put under an argon atmosphere. Dry DMSO (2.2 mL) was added via syringe, and the solution was heated in a microwave for 1h at 180 °C. No reaction was observed via ^{1}H NMR.

Reaction of 4-fluorophenylacetylene (5) with methylamine hydrochloride: 4-fluorophenylacetylene (115.2 mg, 0.96 mmol), methylamine hydrochloride (73.4 mg, 1.09 mmol), and Cs_2CO_3 (1.12 g, 3.7 mmol) were added to a 2.0-5.0 mL Biotage microwave tube, which was sealed and put under an argon atmosphere. Dry NMP (2.7 mL) was added via syringe, and the solution was heated in a microwave for 30 minutes at 220 °C. No reaction was observed via ^{1}H NMR.

Reaction of 4-fluoroacetophenone (8) with ethanol: Sodium hydride (60% dispersion in mineral oil) (133.5 mg, 3.3 mmol) was added to a 2.0-5.0 mL Biotage microwave tube, which was sealed and put under an argon atmosphere. Dry DMSO (2.7 mL), ethanol (60 µL, 1.03 mmol), and 4-fluoroacetophenone (125 µL, 1.0 mmol) were added via syringe, and the solution was heated for 1h at 50 °C. The substitution product was observed via ^{1}H NMR in ca. 75% conversion.

Reaction of 4-fluorophenylacetylene (5) with ethanol: Sodium hydride (60% dispersion in mineral oil) (58.3 mg, 1.46 mmol) was added to a 2.0-5.0 mL Biotage microwave tube, which was sealed and put under an argon atmosphere. Dry DMSO (2.7 mL) and ethanol (90 µL, 1.54 mmol), were added via syringe, and the solution was allowed to stir for 1h. 4-fluorophenylacetylene (124.5 µL, 1.03 mmol) was added via syringe, and the solution was heated for 2h at 50 °C. The substitution product was observed via ^{1}H NMR in ca. 80% conversion.

3.7 Computational Calculations

All computer calculations were performed using Gaussian 09, Revision A.02, supplied by Gaussian, Inc. GaussView 5.0.8 was used for calculation set up and analysis. Calculations were

performed on two HP ProLiant DL380 G5 servers, each with 2x Intel Xeon X5450 processors (3.0 GHz, 12MB L2 cache, 8 cores total per node), 32GB RAM, and 720GB shared network storage, running RedHat Enterprise Linux 5.5 (kernel 2.6.18-164.15.1). Calculations were generally performed by allocating 4 to 7 CPUs and 12 to 28 GB memory to each link.

CCSD calculations were performed excluding triple excitations. MP4 calculations were MP4(SDTQ). IRC calculations were performed at B3LYP/6-311+G(d,p) using between 20 and 100 steps, with frequency calculations being performed every 3 steps. QST3 calculations were performed with force constants being calculated at every point. Berny transition state calculations were performed with force constants being calculated once. All other optimizations were done with no force constants being pre-calculated. SCRF solvation used the polarizable continuum model and used universal force field (UFF) atomic radii, the matrix inversion solution method, a scaled van der Waals surface cavity type, and the GePol cavity algorithm.

REFERENCES

1. Jones, Jr., M. *Organic Chemistry*, 3rd ed.; W. W. Norton: New York, 2005; pp 271, 726.

2. Carey, F. A.; Sundberg, R. J. *Advanced Organic Chemistry, Part B: Reactions and Synthesis*, 5th ed.; Springer Science: New York, 2007; pp 1035-1039.

3. Reusch, W. Reaction of Alkynes. *Virtual Textbook of Organic Chemistry* [Online]; Michigan State University, 1999. http://www.cem.msu.edu/~reusch/VirtualText/addyne1.htm (accessed Mar 5, 2010).

4. Kolb, H. C.; Finn, M. G.; Sharpless, K. B. *Angew. Chem., Int. Ed.* **2001**, *40* (11), 2004-2021.

5. Glaser, C. Untersuchungen über einige Derivate der Zimmtsäure. *Annalen der Chemie und Pharmacie* **1870**, *154*, 137.

6. Hay, A. S. Oxidative Coupling of Acetylenes. II. *J. Org. Chem.* **1962**, *27* (9), 3320-3321.

7. Sonogashira, K.; Tohda, Y.; Hagihara, N. A convenient synthesis of acetylenes: catalytic substitutions of acetylenic hydrogen with bromoalkenes, iodoarenes and bromopyridines. *Tetrahedron Lett.* **1975**, *16* (50), 4467-4470.

8. Dutta, T.; Woody, K. B.; Waton, M. D. Transition-Metal-Free Synthesis of Poly(phenylene Ethynylene)s with Alternating Aryl-Perfluoroaryl Units. *J. Am. Chem. Soc.* **2008**, *130* (2), 452-453.

9. Paventi, M.; Hay, A. S. *Tetrahedron Lett.* **1993**, *34* (60), 999-1002.

10. Hinze, J.; Jaffe, H. H. Electronegativity. I. Orbital Electronegativity of Neutral Atoms. *J. Am. Chem. Soc.* **1962**, *84* (4), 540-546.

11. Hammett, L. P. The Effect of Structure upon the Reactions of Organic Compounds. Benzene Derivatives. *J. Am. Chem. Soc.* **1937**, *59* (1), 96-103.

12. Eaborn, C.; Thompson, R.; Walton, D. R. M. Aromatic Reactivity. Part XLII. Substituent Effects of the Ethynyl Group. *J. Chem. Soc. B* **1969**, 859-861.

13. Exner, O.; Shorter, J., Ed. *Correlation Analysis of Chemical Data*; Plenum Publishing Corp.: Prague, 1988.

14. Hansch, C.; Leo, A.; Taft, R. W. A Survey of Hammett Substituent Constants and Resonance and Field Parameters. *Chem. Rev.* **1991**, *91*, 165-195.

15. Bunnett, J. F. and Zahler, R. E. Aromatic Nucleophilic Substitution Reactions. *Chem. Rev.* **1951**, *49*, 273-412.

16. Bordwell, F. G. Equilibrium acidities in dimethyl sulfoxide solution. *Acc. Chem. Res.* **1988**, *21*, 456-463.

17. Bordwell, F. G.; McCallum, R. J.; Olmstead, W. N. Acidities and hydrogen bonding of phenols in dimethyl sulfoxide. *J. Org. Chem.* **1984**, *49*, 1424-1427.

18. Olmstead, W. N.; Margolin, Z.; Bordwell, F. G. Acidities of water and simple alcohols in dimethyl sulfoxide solution. *J. Org. Chem.* **1980**, *45*, 3295-3299.

19. de Levie, R. *Advanced Excel for scientific data analysis*, 2nd ed.; Oxford University Press: New York, 2004; pp 625.